

Stability transitions and dynamics of mesa patterns near the shadow limit of reaction-diffusion systems in one space dimension

Rebecca McKay and Theodore Kolokolnikov
Department of Mathematics and Statistics, Dalhousie University, Canada

Abstract

We consider a class of one-dimensional reaction-diffusion systems,

$$\begin{cases} u_t = \varepsilon^2 u_{xx} + f(u, w) \\ \tau w_t = D w_{xx} + g(u, w) \end{cases}$$

with homogeneous Neumann boundary conditions on a one dimensional interval. Under some generic conditions on the nonlinearities f, g and in the singular limit $\varepsilon \rightarrow 0$, such a system admits a steady state for which u consists of sharp back-to-back interfaces. For a sufficiently large D and for sufficiently small τ , such a steady state is known to be stable in time. On the other hand, it is also known that in the so-called shadow limit $D \rightarrow \infty$, patterns having more than one interface are unstable. In this paper we analyse in detail the transition between the stable patterns when $D = O(1)$ and the shadow system when $D \rightarrow \infty$. We show that this transition occurs when D is *exponentially large in ε* and we derive instability thresholds $D_1 \gg D_2 \gg D_3 \gg \dots$ such that a periodic pattern with $2K$ interfaces is stable if $D < D_K$ and is unstable when $D > D_K$. We also study the dynamics of the interfaces when D is exponentially large; this allows us to describe in detail the mechanism leading to the instability. Direct numerical computations of stability and dynamics are performed, and these results are in excellent agreement with corresponding results as predicted by the asymptotic theory.

1 Introduction

One of the most prevalent phenomena observed in reaction-diffusion systems is the formation of *mesa patterns*. Such patterns consist of a sequence of highly localized interfaces (or kinks) that are separated in space by regions where the solution is nearly constant. These patterns has been studied intensively for the last three decades and by now an extensive literature exists on this topic. We refer for example to [1, 2, 3, 4, 5, 6, 7, 8, 9, 10] and references therein. In this paper we are concerned with the following class of reaction-diffusion models:

$$\begin{cases} u_t = \varepsilon^2 u_{xx} + f(u, w) \\ 0 = D w_{xx} + g(u, w) \end{cases} \quad (1)$$

where $u, w \in \mathbb{R}$; $t \geq 0$; $x \in (a, b)$, a one-dimensional interval of a finite size, with Neumann boundary conditions and in the limit

$$\varepsilon \ll 1 \quad \text{and} \quad D \gg 1 \quad (2)$$

where all other parameters are assumed to be $O(1)$ independent of ε, D .

Due to the large diffusivity ratio D/ε^2 , and under certain general conditions on the nonlinearities f and g that will be specified below, the system (1) admits a steady state for $u(x)$ which consists of an *interface layer solution*. Such a solution has the property that u is very close to some constants u_+ or u_- with $u_+ \neq u_-$ everywhere except near the interface location, where it has a layer of size $O(\varepsilon)$ connecting the two constant states u_{\pm} . On the other hand, $w(x)$ is nearly constant. A single *mesa* (or a box) solution

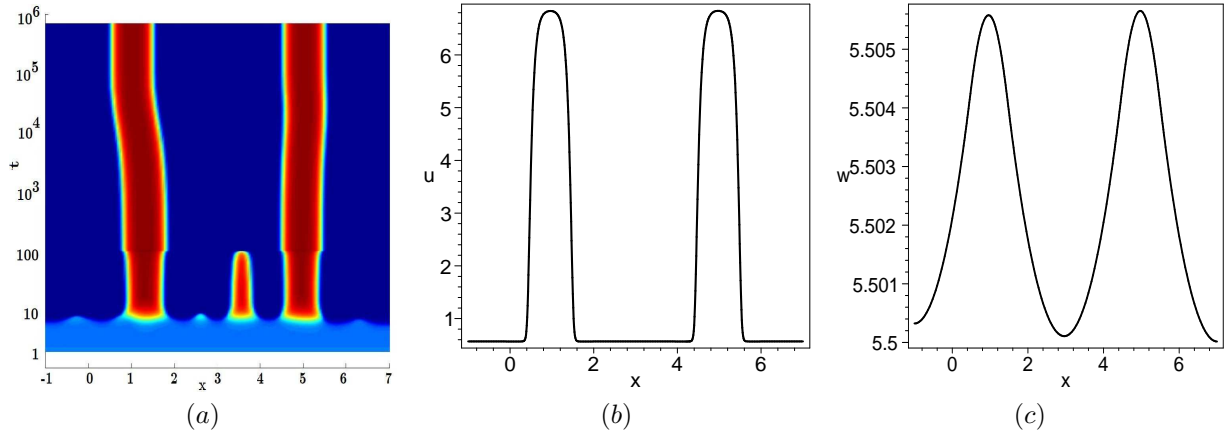


Figure 1: (a) Coarsening process in Lengyel-Epstein model (8), starting with random initial conditions. Time evolution of u is shown; note the logarithmic time scale. The parameter values are $\varepsilon = 0.06$, $a = 10$, $D = 500$, $\tau = 0.1$, domain size is 8 with Neumann boundary conditions for both u and w . (b,c) The snapshots of u and w at $t = 1,000,000$.

consists of two interfaces, one connecting u_- to u_+ and another connecting u_+ back to u_- . By mirror reflection, a single mesa can be extended to a symmetric K mesa solution, consisting of K mesas or $2K$ interfaces (see Figure 1b).

The general system (1) has been thoroughly studied by many authors. In particular, the regime $D = O(1)$ is well understood. Under certain general conditions on g and f , it is known that a K -mesa pattern is stable for all K – see for example [1], [11]. On the other hand, in the limit $D \rightarrow \infty$ and on a finite domain $[a, b]$, the system (1) reduces to the so-called shadow system,

$$u_t = \varepsilon^2 u_{xx} + f(u, w_0); \quad \int_a^b g(u, w_0) dx = 0. \quad (3)$$

where w_0 is a constant. Equation (3) also includes many models of phase separation such as Allen-Cahn [4] as a special case. Under the same general conditions on g and f , a single interface of the shadow system is also stable; however a pattern consisting of more than one interface is known to be unstable [12].

The main question that we address in this paper is how the transition from the stable regime $D = O(1)$ to the unstable shadow regime $D \rightarrow \infty$ takes place. When D is not too large, the stability of a K mesa pattern is due to the stabilizing effect of the global variable w , as shown for example in [1]. However as D is increased, the stabilizing effect of w is decreased, and eventually the pattern loses its stability. We find that the onset of instability is caused by the interaction between the interfaces of u . This interaction is exponentially small, but becomes important as D becomes exponentially large. By analysing the contributions to the stability of both w and u , we compute an explicit sequence of threshold values $D_1 > D_2 > D_3 > \dots$ such that a K mesa solution on the domain of a fixed size $2R$ is stable if $D < D_K$ and is unstable if $D > D_K$. These thresholds have the order $\ln(D_K) = O(\frac{1}{\varepsilon})$, so that D_K is exponentially large in ε .

There are many systems that fall in the class described in this paper. Let us now mention some of them. In the models below the parameters $\beta_0, f_0, q, \kappa, \alpha$ are assumed to be constants.

- **Cubic model:** One of the simplest systems is a cubic model,

$$\begin{cases} u_t = \varepsilon^2 u_{xx} + 2u - 2u^3 + w \\ 0 = Dw_{xx} - u + \beta_0 \end{cases}. \quad (4)$$

It is a variation on FitzHugh-Nagumo model used in [5] and in [13]. It is a convenient model for testing our asymptotic results.

- **Model of Belousov-Zhabotinskii reaction in water-in-oil microemulsion:** This model is a was introduced in [14], [15]. In [16], the following simplified model was analysed in two dimensions:

$$\begin{cases} u_t = \varepsilon^2 u_{xx} - f_0 \frac{u-q}{u+q} + wu - u^2 \\ 0 = Dw_{xx} + 1 - uw \end{cases} . \quad (5)$$

- **Brusselator model.** In [17] the authors considered coarsening phenomenon in the Brusselator model; a self-replication phenomenon was studied in [11]. After a change of variables the Brusselator may written as

$$\begin{cases} u_t = \varepsilon^2 u_{xx} - u + uw - u^3 \\ 0 = Dw_{xx} - \beta_0 u + 1 \end{cases} . \quad (6)$$

- **Gierer-Meinhardt model with saturation.** This model was introduced in [18], (see also [19], [20]) to model stripe patterns on animal skins. After some rescaling, it is

$$\begin{cases} u_t = \varepsilon^2 u_{xx} - u + \frac{u^2}{w(1 + \kappa u^2)} \\ \tau w_t = Dw_{xx} - w + u^2 \end{cases} . \quad (7)$$

This model was also studied in [21], where stripe instability thresholds were computed.

- **Lengyel-Epstein model.** This model was introduced in [22], see also [23]:

$$\begin{cases} u_t = u_{xx} + a - u - \frac{4uv}{1 + u^2} \\ \tau v_t = Dv_{xx} + u - \frac{4uv}{1 + u^2} \end{cases} . \quad (8)$$

- **Other models** include: models for co-existence of competing species [24]; vegetation patterns in dry regions [25]; models of chemotaxis [26] and models of phase separation in diblock copolymers [27].

Note that some of the models such as (7) and (8) are a slight generalization of (1), in that they include a time derivative of w , namely

$$\begin{cases} u_t = \varepsilon^2 u_{xx} + f(u, w) \\ \tau w_t = Dw_{xx} + g(u, w) \end{cases} . \quad (9)$$

All of the results of this paper remain unchanged provided that τ is not too large, in particular $0 < \tau \ll O(1/\varepsilon)$. See Remark 3.5. On the other hand, it can be shown that oscillatory instabilities can and do occur if $\tau = O(D/\varepsilon)$ [28].

Figure 1 illustrates the instability phenomenon studied in this paper, as observed numerically in the Lengyel-Epstein model. Starting with random initial conditions, Turing instability leads to a formation of a three-mesa pattern at $t \approx 10$. However such a pattern is unstable, even though this only becomes apparent much later (at $t \approx 100$). This is due to the very slow instability of a three-mesa pattern. The resulting two-mesa pattern then drifts towards a symmetric position which is stable. Note that the component u consists of a sequence of localized interfaces that connects $u_- \approx 0.57$ to $u_+ \approx 6.84$; on the other hand w is nearly constant with $w \approx 5.50$. Also note that the top of the mesa pattern is not completely flat: there is some (weak) interaction between the two interfaces making up the mesa. The relative strength of such interaction is what effectively determines the stability of a pattern.

A similar phenomenon for the Belousov-Zhabotinskii model (5) is illustrated in Figure 7(b). It shows the time-evolution a 2-mesa solution to (5) with $D > D_2$, starting with initial conditions that consist of a slightly perturbed two-mesa pattern. After a very long time, one of the mesas absorbs the mass of the

other. The surviving mesa then moves towards the center of the domain where it remains as a stable pattern.

In addition to studying the stability of the mesa patterns, we also study their dynamics. This allows us to describe in detail the mechanism by which the exchange of mass between two mesas can take place, as well as the motion of the interfaces away from the equilibrium. For a pattern consisting of K mesas, we derive a *reduced problem*, consisting of $2K$ ODE's that govern the asymptotic motion of the $2K$ interfaces.

The results in this paper are derived using the methods of formal asymptotics. It is a difficult challenge to provide a rigorous justification, especially due to the presence of exponentially small and large terms, and we have not attempted to do so. However extensive numerics were used to verify the asymptotic results. As will be shown in §5, the agreement between the numerics and the analytical theory is excellent, even for relatively large values of ε (for example less than 1% error when $\varepsilon = 0.2$ for certain problems). The effectiveness of our theory even for moderate values of ε is one of the key unanticipated successes of asymptotic analysis.

The outline of the paper is as follows. In §2 we construct the steady state consisting of K mesas. The construction is summarized in Proposition 2.1. The main result is presented in §3 (Principal Result 3.1), where we analyse the asymptotics of the linearized problem for the periodic pattern, and derive the instability thresholds D_K . In §4 we derive the reduced equations of motion for the interfaces. In §5 we present numerical computations to support our asymptotic results. We conclude with a discussion of open problems in §6.

2 Preliminaries: construction of the K -mesa steady state

We start by constructing the time-independent mesa-type solution to (1). The mesa (or box) solution consists of two back-to-back interfaces. Thus we first consider the conditions for existence of a single interface solution and review its construction. A mesa solution can then be constructed from a single interface by reflecting and doubling the domain size. Similarly, a K -mesa pattern is then constructed by making K copies of a single mesa. We summarize the construction as follows.

Proposition 2.1 *Consider the time-independent steady state of the PDE system (1) satisfying*

$$\begin{cases} 0 = \varepsilon^2 u_{xx} + f(u, w) \\ 0 = Dw_{xx} + g(u, w) \end{cases} \quad (10)$$

with Neumann boundary conditions and in the limit

$$\varepsilon \ll 1 \quad \text{and} \quad D \gg 1. \quad (11)$$

Suppose that the algebraic system

$$\int_{u_-}^{u_+} f(u, w_0) du = 0; \quad f(u_+, w_0) = 0 = f(u_-, w_0) \quad (12)$$

admits a solution u_+, u_-, w_0 , with $u_+ \neq u_-$. Define

$$g_{\pm} := g(u_{\pm}, w_0) \quad (13)$$

and suppose in addition that

$$f_u(u_{\pm}, w_0) < 0 \quad \text{and} \quad 0 < \frac{g_-}{g_- - g_+} < 1. \quad (14)$$

Then a single interface solution, on the interval $[0, L]$ is given by

$$u(x) \sim U_0 \left(\frac{x-l}{\varepsilon} \right), \quad w \sim w_0 \quad (15)$$

where U_0 is the heteroclinic connection between u_+ and u_- satisfying

$$\begin{cases} U_{0yy} + f(U_0, w_0) = 0; \\ U_0 \rightarrow u_- \text{ as } y \rightarrow \infty; \quad U_0 \rightarrow u_+ \text{ as } y \rightarrow -\infty; \\ f(U_0(0), w_0) = 0 \end{cases} \quad (16)$$

and l is the location of the interface so that

$$u \sim \begin{cases} u_+, & 0 < x < l \\ u_-, & l < x < L \end{cases}.$$

Moreover, l satisfies

$$l = l_0 + \varepsilon l_1 + O(\varepsilon^2) \quad (17)$$

where

$$l_0 = \frac{g_-}{g_- - g_+} L \quad (18)$$

and

$$l_1 = \frac{\int_0^\infty [g(U_0(y), w_0) - g_-] dy + \int_{-\infty}^0 [g(U_0(y), w_0) - g_+] dy}{g_- - g_+} \quad (19)$$

A single mesa solution on the interval $[-L, L]$ is obtained by even reflection of the interface solution on an interval $[0, L]$ around $x = 0$. A K -mesa solution on the interval of size $2KL$ is then obtained making K copies of the single mesa solution on the interval $[-L, L]$.

For future reference, we also define

$$\mu_\pm := \sqrt{-f_u(u_\pm, w_0)} \geq 0; \quad (20)$$

and define constants C_\pm to be such that

$$\begin{aligned} U_0(y) &\sim u_- + C_- e^{-\mu_- y}, & y \rightarrow +\infty; \\ U_0(y) &\sim u_+ - C_+ e^{\mu_+ y}, & y \rightarrow -\infty. \end{aligned} \quad (21)$$

The constants $C_\pm > 0$ are known constants determined by the far-field behavior of the heteroclinic solution $U_0(y)$.

We note that the assumption $D \gg 1$ implies that to leading order, $w \sim w_0$ throughout the interval. In particular, the equation (15) is valid throughout the whole interval and not just near the boundary layer; that is, $|u(x) - U_0(\frac{x-l}{\varepsilon})| < C \max(\varepsilon, \frac{1}{D})$ and $|w(x) - w_0| \leq \frac{C}{D}$ for some constant C and for all x in the domain of definition. More generally, the construction of the steady state can be generalized under a weaker assumption $\varepsilon^2 \ll D = O(1)$. In this case, $w \sim w_0$ within the interface layer but has an x dependence in the outer region, away from the interface layer [1], [8], [11]; and (15) would be valid only near the interface, $|x - l| \ll \varepsilon$. However as was shown in [1] (see also [11]), the K -mesa pattern is stable when $D = O(1)$. Since we are concerned about transitions to instability, we only consider the case $D \gg O(1)$ here.

The construction in Proposition 2.1 is straightforward and we outline its derivation here. First, consider a single interface located at $x = l$ inside the domain $[0, L]$. We assume that $u \sim u_+$ for $0 < x < l$ and $u \sim u_-$ for $l < x < L$ where u_\pm are constants to be determined. Since we assumed that $D \gg 1$, we expand

$$w = w_0 + \frac{1}{D} w_1 + \dots$$

so that to leading order $w \sim w_0$ is constant. Near the interface we introduce inner variables

$$x = l + \varepsilon y; \quad u(x) \sim U_0\left(\frac{x-l}{\varepsilon}\right), \quad w \sim w_0. \quad (22)$$

Then $U_0(y)$ satisfies the system (16) which is parametrized by w_0 . In order for such a solution to exist, u_\pm must both be roots of $f(u, w_0) = 0$ and U_0 must be a heteroclinic orbit connecting u_+ and u_- . This

yields the three algebraic constraints (12) which determine u_{\pm} and w_0 . To determine the location l of the interface, we integrate the second equation in (1), and using Neumann boundary conditions we obtain

$$\int_0^L g(u, w_0) dx = 0.$$

Changing variables $x = l + \varepsilon y$ we estimate

$$\begin{aligned} 0 &\sim \varepsilon \int_{-l/\varepsilon}^0 g(U_0(y), w_0) dy + \varepsilon \int_0^{(L-l)/\varepsilon} g(U_0(y), w_0) dy; \\ 0 &\sim l g_+ + \varepsilon \int_{-\infty}^0 [g(U_0(y), w_0) - g_+] dy + (L-l) g_- + \varepsilon \int_0^{\infty} [g(U_0(y), w_0) - g_-] dy \end{aligned}$$

Expanding l in ε as in (17) then yields (18) and (19). Since we must have $0 < l < L$, this yields an additional constraint (14).

3 Stability of K -mesa pattern

We now state the main result of this paper.

Principal Result 3.1 *Consider the steady state consisting of K mesas on the interval of size $2KL$, with Neumann boundary conditions, as constructed in Proposition 2.1, in the limit $\varepsilon \rightarrow 0$. Suppose that*

$$\left(g_w - g_u \frac{f_w}{f_u} \right)_{\substack{u=u_{\pm}, \\ w=w_0}} < 0 \quad \text{and} \quad (g_- - g_+) \int_{u_-}^{u_+} f_w du > 0. \quad (23)$$

Let

$$\alpha_+ := \frac{2C_+^2 \mu_+^3}{\int_{u_-}^{u_+} f_w du} \frac{1}{\varepsilon} \exp\left(-\frac{2\mu_+ l}{\varepsilon}\right); \quad \alpha_- := \frac{2C_-^2 \mu_-^3}{\int_{u_-}^{u_+} f_w du} \frac{1}{\varepsilon} \exp\left(-\frac{2\mu_- (L-l)}{\varepsilon}\right) \quad (24)$$

where the constants C_{\pm}, μ_{\pm}, l are as defined in Proposition 2.1.

Define

$$D_1 := \frac{Lg_-^2}{2(g_- - g_+) \alpha_-} = \frac{l_0 g_-}{2\alpha_-}; \quad (25)$$

$$D_1^i := \frac{Lg_+^2}{2(g_- - g_+) \alpha_+} = \frac{(L-l_0) g_+}{2\alpha_+}; \quad (26)$$

and for $K \geq 2$, define

$$D_K := \begin{cases} D_1 & \text{if } \mu_-(L-l_0) < \mu_+ l_0 \\ D_1^i & \text{if } \mu_-(L-l_0) > \mu_+ l_0 \\ \frac{L}{2(g_- - g_+) (g_+^2 \alpha_+ + g_-^2 \alpha_-)} \left(\frac{1}{2} + \sqrt{\frac{1}{4} - \frac{2\alpha_+ \alpha_- (1 - \cos \pi/K) g_+^2 g_-^2}{4(g_+^2 \alpha_+ + g_-^2 \alpha_-)^2}} \right)^{-1} & \text{if } \mu_-(L-l_0) = \mu_+ l_0. \end{cases} \quad (27)$$

Then the K mesa pattern is a stable equilibrium of the time-dependent system (1) if $D < D_K$, and is unstable if $D > D_K$.

Principal Result 3.1 follows from a detailed study of the linearization about the steady state. We consider small perturbations of the steady state of the form

$$u(x, t) = u(x) + \phi(x) e^{\lambda t}, \quad w(x, t) = w(x) + \psi(x) e^{\lambda t}$$

where $u(x), w(x)$ denotes the K -mesa equilibrium solution of (10) on the interval of length $2KL$ with Neumann boundary conditions, whose leading order asymptotic profile was constructed in Proposition 2.1. For small perturbations ϕ, ψ we get the following eigenvalue problem,

$$\begin{cases} \lambda\phi = \varepsilon^2\phi'' + f_u(u, w)\phi + f_w(u, w)\psi \\ 0 = D\psi'' + g_u(u, w)\phi + g_w(u, w)\psi \end{cases} \quad (28)$$

with Neumann boundary conditions. The sign of the real part of the eigenvalue λ determines the linear stability: the system is said to be linearly unstable if there exists a solution to (28) with $\text{Re}(\lambda) > 0$; it is linearly stable if $\text{Re}(\lambda) < 0$ for all solutions λ to (28).

Remark 3.2 *As will be shown in Lemma 3.6, the conditions (23) guarantee that a single interface is stable for any $D \gg 1$: they imply that $\lambda_{\text{even}} < 0$ where λ_{even} is given by (57). In addition, second condition in (23) guarantees that $\lambda_{\text{odd}} < 0$ whenever $1 \ll \ln D \ll 1/\varepsilon$, where λ_{odd} is given by (56). Taken together, the conditions (23) are precisely those that guarantee the stability of a single mesa whenever $1 \ll \ln D \ll 1/\varepsilon$.*

To determine the threshold conditions for stability under Neumann boundary conditions, we first consider the case of periodic boundary conditions. One key ingredient in the analysis below is featured in the following Lemma:

Lemma 3.3 (Periodic boundary conditions) *Consider the steady state consisting of K mesas on the interval of size $2KL$, as constructed in Proposition 2.1, and consider the linearized problem (28) with periodic boundary conditions*

$$\phi(-L) = \phi(2KL - L), \quad \phi'(-L) = \phi'(2KL - L); \quad \psi(-L) = \psi(2KL - L), \quad \psi'(-L) = \psi'(2KL - L).$$

The linearized problem admits $2K$ eigenvalues. Of these, $2K - 2$ are given asymptotically by

$$\lambda_\theta^\pm \sim (a \pm |b|) \frac{\varepsilon \int_{u_-}^{u_+} f_w du}{\int_{-\infty}^{\infty} U_{0y}^2 dy} \quad (29)$$

where

$$a = \alpha_+ + \alpha_- + \frac{(g_+ - g_-)}{D} \frac{L}{1 - \cos\theta} - \frac{g_+ l_0}{D} \quad (30)$$

$$\begin{aligned} |b|^2 = & \alpha_+^2 + \alpha_-^2 + 2\alpha_+\alpha_- \cos\theta + \frac{2(g_+ - g_-)}{D} \left[\frac{L(\alpha_+ + \alpha_-)}{1 - \cos\theta} - l_0\alpha_+ - (L - l_0)\alpha_- \right] \\ & + \frac{(g_+ - g_-)^2}{D^2(1 - \cos\theta)^2} [L^2 - 2(1 - \cos\theta)l_0(L - l_0)] \end{aligned} \quad (31)$$

with α_\pm given by (24) and

$$\theta = 2\pi k/K; \quad k = 1 \dots K - 1. \quad (32)$$

The other two eigenvalues are $\lambda = 0$ (for which the corresponding eigenfunction is $(\phi, \psi) = (u_x, w_x)$) and

$$\lambda_{\text{even}} \sim - \frac{g_+ - g_-}{\sigma_+ l_0 + \sigma_- (L - l_0)} \frac{\varepsilon \int_{u_-}^{u_+} f_w du}{\int_{-\infty}^{\infty} U_{0y}^2 dy} \quad (33)$$

where $\sigma_\pm < 0$ are given by

$$\sigma_\pm \equiv \left(g_w - g_u \frac{f_w}{f_u} \right) \Big|_{u=u_\pm, w=w_0}. \quad (34)$$

Remark 3.4 Note that if $\theta = \pi$ and recalling (18), the equations (30) and (31) simplify to

$$|b| = \left| \frac{L}{2D} \frac{g_+^2 - g_-^2}{g_+ - g_-} + \alpha_+ - \alpha_- \right|; \quad a = \alpha_+ + \alpha_- + \frac{L}{2D} \frac{g_+^2 + g_-^2}{g_+ - g_-}.$$

Therefore the formula (29) simplifies as follows: If $|b| = b$ then

$$\lambda_\pi^- = \left(2\alpha_- - \frac{g_-^2 L}{D(g_- - g_+)} \right) \frac{\varepsilon \int_{u_-}^{u_+} f_w du}{\int_{-\infty}^{\infty} U_{0y}^2 dy}; \quad \lambda_\pi^+ = \left(2\alpha_+ - \frac{g_+^2 L}{D(g_- - g_+)} \right) \frac{\varepsilon \int_{u_-}^{u_+} f_w du}{\int_{-\infty}^{\infty} U_{0y}^2 dy} \quad (35)$$

Otherwise λ_π^\pm are given by (35) except that λ_π^+ and λ_π^- are interchanged.

Derivation of Lemma 3.3. The idea is to make use of Floquet theory. That is, instead of considering (28) with periodic boundary conditions on $[-L, 2KL - L]$, we consider (28) on the interval $[-L, L]$ with the boundary conditions

$$\phi(L) = z\phi(-L), \quad \phi'(L) = z\phi'(-L); \quad \psi(L) = z\psi(-L), \quad \psi'(L) = z\psi'(-L), \quad (36)$$

We then extend such a solution to the interval $[L, 3L]$ by defining $\phi(x) := z\phi(x - 2L)$ for $x \in [L, 3L]$ and similarly for ψ . This extension assures continuity of ϕ, ψ and ϕ', ψ' at L . Moreover, since u, w are periodic with period $2L$, it is clear that ϕ, ψ extended in this way satisfies (28) on $[-L, 3L]$ and moreover $\phi(3L) = z^2\phi(-L)$. Repeating this process, we obtain solution of (28) on the whole interval $[-L, 2KL - L]$ with $\phi(2KL - L) = \phi(-L)z^K$. Hence, by choosing

$$z = \exp(2\pi ik/K), \quad k = 0 \dots K - 1,$$

we have obtained a periodic solution to (28) on $[-L, 2KL - L]$.

To solve (28) on $[-L, L]$ subject to (36), we estimate the eigenfunctions as

$$\phi \sim c_\pm u_x; \quad \psi \sim \psi(\pm l) \quad \text{when } x \sim \pm l. \quad (37)$$

Note that

$$0 = \varepsilon^2 u_{xxx} + f_u u_x + f_w w_x.$$

Multiplying the equation for ϕ in (28) by u_x and integrating by parts on $[-L, 0]$ we then obtain

$$\lambda c_- \int_{-L}^0 u_x^2 dx \sim \varepsilon^2 (\phi_x u_x - \phi u_{xx})_{-L}^0 + \int_{-L}^0 f_w (\psi u_x - \phi w_x) dx$$

We note that the integral term on the right hand side is dominated by the contribution from $x = -l$. Using the ansatz (37) we then obtain

$$\lambda c_- \int_{-L}^0 u_x^2 dx \sim \varepsilon^2 (\phi_x u_x - \phi u_{xx})_{-L}^0 + (\psi(-l) - c_- w_x(-l)) \int_{u_-}^{u_+} f_w du \quad (38)$$

Similarly on the interval $[0, L]$ we get

$$\lambda c_+ \int_0^L u_x^2 dx \sim \varepsilon^2 (\phi_x u_x - \phi u_{xx})_0^L - (\psi(+l) - c_+ w_x(-l)) \int_{u_-}^{u_+} f_w du \quad (39)$$

We estimate

$$\int_0^L u_x^2 dx \sim \int_{-L}^0 u_x^2 dx \sim \frac{1}{\varepsilon} \int_{-\infty}^{\infty} U_{0y}^2 dy$$

and write (38) and (39) as

$$\lambda \kappa_0 \begin{pmatrix} c_+ \\ c_- \end{pmatrix} = \begin{pmatrix} \kappa_1 (-\phi u_{xx})_0^L - \psi(+l) + c_+ w_x(+l) \\ \kappa_1 (-\phi u_{xx})_{-L}^0 + \psi(-l) - c_- w_x(-l) \end{pmatrix} \quad (40)$$

where

$$\kappa_0 = \frac{\int_{-\infty}^{\infty} U_{0y}^2 dy}{\varepsilon \int_{u_-}^{u_+} f_w du}; \quad \kappa_1 = \frac{\varepsilon^2}{\int_{u_-}^{u_+} f_w du}.$$

We now transform (40) into a matrix eigenvalue problem. To do so, we will express the boundary terms as well as $\psi(\pm l)$ in terms of c_{\pm} .

Determining $\psi(\pm l)$. We start by estimating

$$\begin{aligned} \int_{-l^-}^{-l^+} g_u u_x dx &\sim \int_{u_-}^{u_+} g_u du \sim g_+ - g_-; \\ \int_{+l^-}^{+l^+} g_u u_x dx &\sim \int_{u_+}^{u_-} g_u du \sim g_- - g_+ \end{aligned}$$

where $\int_{\pm l^-}^{\pm l^+}$ denotes integration over any interval that includes $\pm l$ and $g_{\pm} = g(u_{\pm}, w_0)$. On the other hand, ϕ is dominated by the contribution from the interfaces. Hence we estimate

$$g_u \phi \sim c_- (g_+ - g_-) \delta(x + l) + c_+ (g_- - g_+) \delta(x - l) \quad (41)$$

where δ is the delta function. Therefore from the equation for ψ in (28) we write

$$\psi(x) \sim -\frac{(g_+ - g_-)}{D} (c_- \eta(x; -l) - c_+ \eta(x; l))$$

where $\eta(x; x_0)$ is a Green's function which satisfies

$$\eta'' + \frac{\sigma(x)}{D} \eta = \delta(x - x_0) \quad (42)$$

with boundary conditions

$$\eta(L) = z\eta(-L), \quad \eta'(L) = z\eta'(-L), \quad z = \exp(2\pi ik/2K), \quad k = 0 \dots K-1 \quad (43)$$

where

$$\sigma(x) \equiv \begin{cases} \sigma_+, & |x| < l \\ \sigma_-, & l < |x| < L \end{cases}; \quad \sigma_{\pm} \equiv \left(g_w - g_u \frac{f_w}{f_u} \right) \Big|_{u=u_{\pm}, w=w_0}. \quad (44)$$

with $\sigma_{\pm} < 0$ by the assumption (23).

There are two distinct cases to consider: either $z = 1$ or $z \neq 1$. For the case $z = 1$, we will show below that there is a large solution of $\eta = O(D)$ that depends on σ at the leading order. On the other hand, if $z \neq 1$ then we expand $\eta = \eta_0 + \frac{1}{D}\eta_1 + \dots$. The boundary terms in (40) will come at the same order as η_0 and the correction terms $\frac{1}{D}\eta_1 + \dots$ may therefore be discarded. The leading order for η then satisfies, after dropping the subscript $\eta_0 = \eta$,

$$\eta_{xx} = 0; \quad \eta(x_0^-; x_0) = \eta(x_0^+; x_0); \quad \eta'(x_0^+; x_0) - \eta'(x_0^-; x_0) = 1$$

so that

$$\eta \sim \begin{cases} A + (x + L)B, & x < x_0 \\ A + (L + x_0)B + (1 + B)(x - x_0), & x > x_0 \end{cases}.$$

The constants A, B are to be chosen so that the boundary conditions (36) are satisfied:

$$A + 2BL + L - x_0 = zA; \quad 1 + B = zB$$

We then obtain

$$B = \frac{z-1}{(z-1)^2}; \quad A = \frac{2L + (L - x_0)(z-1)}{(z-1)^2}$$

$$\eta(l; l) = \eta(-l; -l) = \frac{2Lz}{(z-1)^2}; \quad (45)$$

$$\eta(l; -l) = \frac{2Lz + 2zl(z-1)}{(z-1)^2}; \quad (46)$$

$$\eta(-l; l) = \frac{2Lz + 2l(1-z)}{(z-1)^2} = \overline{\eta(l; -l)}.$$

In summary, we obtain

$$\begin{pmatrix} \psi(l) \\ -\psi(-l) \end{pmatrix} \sim \frac{(g_+ - g_-)}{D} \begin{pmatrix} \eta(l; l) & -\eta(l; -l) \\ -\eta(l; -l) & \eta(l; l) \end{pmatrix} \begin{pmatrix} c_+ \\ c_- \end{pmatrix} \quad (47)$$

where $\eta(l; l)$, $\eta(l; -l)$ are given by (45) and (46), and the overbar denotes complex conjugate.

Boundary terms. Next we compute the boundary terms in (38, 39), corresponding to the behaviour of ϕ at $x = \pm L, 0$. We start by estimating the behaviour of u_x and ϕ near $-L$. Since $u_x(-L) = 0$, we have

$$u \sim u_- + A [\exp(\mu_- z) + \exp(-\mu_- z)], \quad z = \frac{x+L}{\varepsilon}. \quad (48)$$

The constant A is found by matching u to the heteroclinic solution as x :

$$\begin{aligned} U_0(y) &\sim u_- + C_- \exp(\mu_- y); \\ u(x) &\sim U_0\left(\frac{x+L}{\varepsilon}\right) \sim u_- + C_- \exp\left(\mu_- \frac{x+L}{\varepsilon}\right). \end{aligned} \quad (49)$$

Matching (48) and (49) we then obtain

$$A = C_- \exp\left(-\frac{\mu_-}{\varepsilon}(L-l)\right).$$

Performing a similar analysis at $x = 0$ and at $x = L$ we get:

$$u_{xx}(\pm L) = 2C_- \frac{\mu_-^2}{\varepsilon^2} \exp\left(-\frac{\mu_-}{\varepsilon}(L-l)\right); \quad u_{xx}(0) = -2C_+ \frac{\mu_+^2}{\varepsilon^2} \exp\left(-\frac{\mu_+}{\varepsilon}l\right).$$

Next we estimate $\phi(-L)$. Near $x \sim -L$ we write

$$\phi = C_1 \exp\left(\frac{\mu_-}{\varepsilon}(x+L)\right) + C_2 \exp\left(-\frac{\mu_+}{\varepsilon}(x+L)\right)$$

where C_1 and C_2 are to be determined. Away from $-L$, we have $\phi \sim c_- u_x$. Matching the decay modes, we then obtain

$$C_1 = c_- C_- \frac{\mu_-}{\varepsilon} \exp\left(-\frac{\mu_-}{\varepsilon}(L-l)\right).$$

On the other hand, near $x \sim +L$ we write

$$\phi = C_3 \exp\left(\frac{\mu_-}{\varepsilon}(x+L)\right) + C_4 \exp\left(-\frac{\mu_+}{\varepsilon}(x+L)\right);$$

as before, we get

$$C_4 = -c_+ C_+ \frac{\mu_+}{\varepsilon} \exp\left(-\frac{\mu_+}{\varepsilon}(L-l)\right).$$

The constants C_2 and C_3 are determined by using the boundary conditions (43), which yields

$$C_3 = zC_1; \quad C_4 = zC_2$$

In summary, we get

$$\begin{aligned} \phi(-L) &\sim C_- \frac{\mu_-}{\varepsilon} \exp\left(-\frac{\mu_-}{\varepsilon}(L-l)\right) \left[c_- - \frac{1}{z} c_+ \right]; \\ \phi(L) &\sim C_- \frac{\mu_-}{\varepsilon} \exp\left(-\frac{\mu_-}{\varepsilon}(L-l)\right) [z c_- - c_+]. \end{aligned}$$

Performing a similar analysis at $x \sim 0$, we obtain

$$\phi(0) \sim C_+ \frac{\mu_+}{\varepsilon} \exp\left(-\frac{\mu_+ l}{\varepsilon}\right) [c_- - c_+].$$

We thus obtain

$$\begin{aligned} (\phi u_{xx})_0^L &= 2C_-^2 \frac{\mu_-^3}{\varepsilon^3} \exp\left(-\frac{2\mu_-}{\varepsilon}(L-l)\right) [zc_- - c_+] + 2C_+^2 \frac{\mu_+^3}{\varepsilon^3} \exp\left(-\frac{2\mu_+}{\varepsilon}l\right) [c_- - c_+]; \\ (\phi u_{xx})_{-L}^0 &= -2C_-^2 \frac{\mu_-^3}{\varepsilon^3} \exp\left(-\frac{2\mu_-}{\varepsilon}(L-l)\right) \left[c_- - \frac{1}{z}c_+\right] - 2C_+^2 \frac{\mu_+^3}{\varepsilon^3} \exp\left(-\frac{2\mu_+}{\varepsilon}l\right) [c_- - c_+]; \end{aligned}$$

so that

$$\begin{bmatrix} \kappa_1 (\phi_x u_x - \phi u_{xx})_0^L \\ \kappa_1 (\phi_x u_x - \phi u_{xx})_{-L}^0 \end{bmatrix} = \begin{bmatrix} \alpha_+ + \alpha_- & -\alpha_+ - z\alpha_- \\ -\alpha_+ - \frac{1}{z}\alpha_- & \alpha_+ + \alpha_- \end{bmatrix} \begin{bmatrix} c_+ \\ c_- \end{bmatrix} \quad (50)$$

where α_{\pm} are given by (24).

Finally, we estimate

$$w'(l) \sim -\frac{g_+ l}{D} \sim -w'(-l). \quad (51)$$

Substituting (50), (51) and (47) into (40) we obtain

$$\lambda \kappa_0 \begin{pmatrix} c_+ \\ c_- \end{pmatrix} = \begin{pmatrix} a & b \\ \bar{b} & a \end{pmatrix} \begin{pmatrix} c_+ \\ c_- \end{pmatrix}$$

where

$$a = \alpha_+ + \alpha_- + \frac{(g_- - g_+)}{D} \eta(l; l) - \frac{g_+ l}{D}; \quad b = -\alpha_+ - z\alpha_- - \frac{(g_- - g_+)}{D} \eta(l; -l).$$

It follows that

$$\lambda \kappa_0 = a \pm |b|.$$

Next we compute

$$\begin{aligned} a &= \alpha_+ + \alpha_- + \frac{2(g_- - g_+)}{D} \frac{Lz}{(z-1)^2} - \frac{g_+ l}{D} \\ b &= -\alpha_+ - z\alpha_- - \frac{2(g_- - g_+)}{D} \frac{Lz + zl(z-1)}{(z-1)^2} \\ \bar{b} &= -\alpha_+ - \frac{1}{z}\alpha_- - \frac{2(g_- - g_+)}{D} \frac{Lz - l(z-1)}{(z-1)^2} \\ |b|^2 &= \alpha_+^2 + \alpha_-^2 + \alpha_+ \alpha_- (z + \bar{z}) + \alpha_+ \frac{2(g_- - g_+)}{D} \left(\frac{2Lz}{(z-1)^2} + l \right) + \alpha_- \frac{2(g_- - g_+)}{D} \left(\frac{L(z^2 + 1)}{(z-1)^2} - l \right) \\ &\quad + \frac{4(g_- - g_+)^2}{D^2} \left(\frac{z^2 L^2}{(z-1)^4} + \frac{zl(L-l)}{(z-1)^2} \right) \end{aligned}$$

We write

$$z = e^{i\theta}, \quad \phi = 2\pi k/K$$

and note that

$$\frac{2z}{(z-1)^2} = \frac{1}{\cos\theta - 1}; \quad \frac{(z^2 + 1)}{(z-1)^2} = \frac{\cos\theta}{\cos\theta - 1}.$$

Combining these computations, we obtain (29), (30), (31), provided that $z \neq 1$.

Next we consider (36) with $z = 1$, which corresponds to periodic boundary conditions on $[-L, L]$. This admits two solutions. One is $\lambda = 0$ corresponding the odd eigenfunction $\phi = u_x, \psi = w_x$. The other eigenfunction is even. This corresponds to imposing the boundary conditions

$$\phi'(0) = 0 = \phi'(L); \quad \psi'(0) = 0 = \psi'(L).$$

As before, we assume

$$\phi \sim u_x; \quad \psi \sim \psi(l) \quad \text{when } x \sim l. \quad (52)$$

and obtain

$$\lambda \int_0^L u_x^2 dx \sim \varepsilon^2 (\phi_x u_x - \phi u_{xx})_0^L - (\psi(l) - w_x(l)) \int_{u_-}^{u_+} f_w du \quad (53)$$

As before, we obtain

$$\psi(x) \sim \frac{(g_+ - g_-)}{D} \eta(x; l)$$

where $\eta(x; x_0)$ satisfies (42) with boundary conditions $\eta'(0) = 0 = \eta'(L)$. We then obtain

$$\eta \sim \frac{D}{\int_0^L \sigma(x) dx} \sim \frac{D}{\sigma_+ l + \sigma_- (L - l)}.$$

Therefore $\psi(l) = O(1) \gg w_x(l) = O(1/D)$ and we estimate

$$\psi(l) - w_x(l) \sim \frac{(g_+ - g_-)}{\sigma_+ l + \sigma_- (L - l)}.$$

The boundary term is evaluated as previously, but is of smaller order. This yields the formula (33) for the even eigenvalue. ■

Remark 3.5 *All the results of this paper remain unchanged if (1) is generalized to (9) provided that $0 \leq \tau \ll O(1/\varepsilon)$ while other conditions remain unchanged. This is seen as follows. The addition of the τw_t term has the effect of changing (44) to*

$$\sigma(x) \equiv \begin{cases} \sigma_+, & |x| < l \\ \sigma_-, & l < |x| < L \end{cases}; \quad \sigma_{\pm} \equiv -\lambda\tau + \left(g_w - g_u \frac{f_w}{f_u} \right) \Big|_{u=u_{\pm}, w=w_0}. \quad (54)$$

To leading order, this is equal to (44) as long as $\lambda\tau \ll 1$; in that case the remaining computations are unchanged, and the end result is that $\lambda_{\text{even}} = O(\varepsilon)$ while all other eigenvalues are of order $O(\frac{\varepsilon}{D}) \ll O(\varepsilon)$. Therefore the results remains unchanged provided that $0 \leq \tau \ll O(1/\varepsilon)$.

We now use Lemma 3.3 to characterize stability with Neumann boundary conditions as follows. Suppose that ϕ has Neumann boundary conditions on $[0, a]$. Then we may extend ϕ by even reflection around the origin; it then becomes periodic on $[-a, a]$. The same argument applies to ψ . From this principle, it follows that the eigenvalues of a K mesa steady state with Neumann boundary conditions form a subset of the eigenvalues of $2K$ mesas with periodic boundary conditions. On the other hand, if ϕ, ψ is an eigenfunction on $[-a, a]$ with periodic boundary conditions then so is $\phi(-x)$ and hence $\hat{\phi}(x) = \phi(x) + \phi(-x)$, $\hat{\psi}(x) = \psi(x) + \psi(-x)$ is an eigenfunction on $[0, a]$ with Neumann boundary conditions, provided that at least one of $\hat{\psi}(x)$, $\hat{\phi}(x) \neq 0$ for some $x \in [0, a]$. Since $\hat{\phi}'(0) = \hat{\psi}'(0) = 0$ and ϕ, ψ satisfies a 2nd order ODE we have that $\hat{\phi}, \hat{\psi} \neq 0$ iff $\hat{\phi}(0) \neq 0$ or $\hat{\psi}(0) \neq 0$; iff $\phi(0) \neq 0$ or $\psi(0) \neq 0$. Verifying this condition, we obtain the following result.

Lemma 3.6 (Neumann boundary conditions) *Consider the steady state consisting of K mesas on the interval of size $2KL$, with Neumann boundary conditions. The linearized problem admits $2K$ eigenvalues. Of these, $2K - 2$ are given asymptotically by (29, 30, 31) of Lemma 3.3, but with*

$$\theta = \pi k/K, \quad k = 1 \dots K - 1. \quad (55)$$

The additional two eigenvalues correspond to an even and odd eigenfunction with Neumann boundary conditions on $[-L, +L]$. They are

$$\lambda_{\text{odd}} = \frac{\varepsilon}{D} \left(2\alpha_- D - \frac{g_-^2 L}{(g_- - g_+)} \right) \frac{\int_{u_-}^{u_+} f_w du}{\int_{-\infty}^{\infty} U_{0y}^2 dy} \quad (56)$$

$$\lambda_{\text{even}} = -\varepsilon \frac{g_+ - g_-}{\sigma_+ l + \sigma_- (L - l)} \frac{\int_{u_-}^{u_+} f_w du}{\int_{-\infty}^{\infty} U_{0y}^2 dy} \quad (57)$$

with all the symbols as defined in Lemma 3.3.

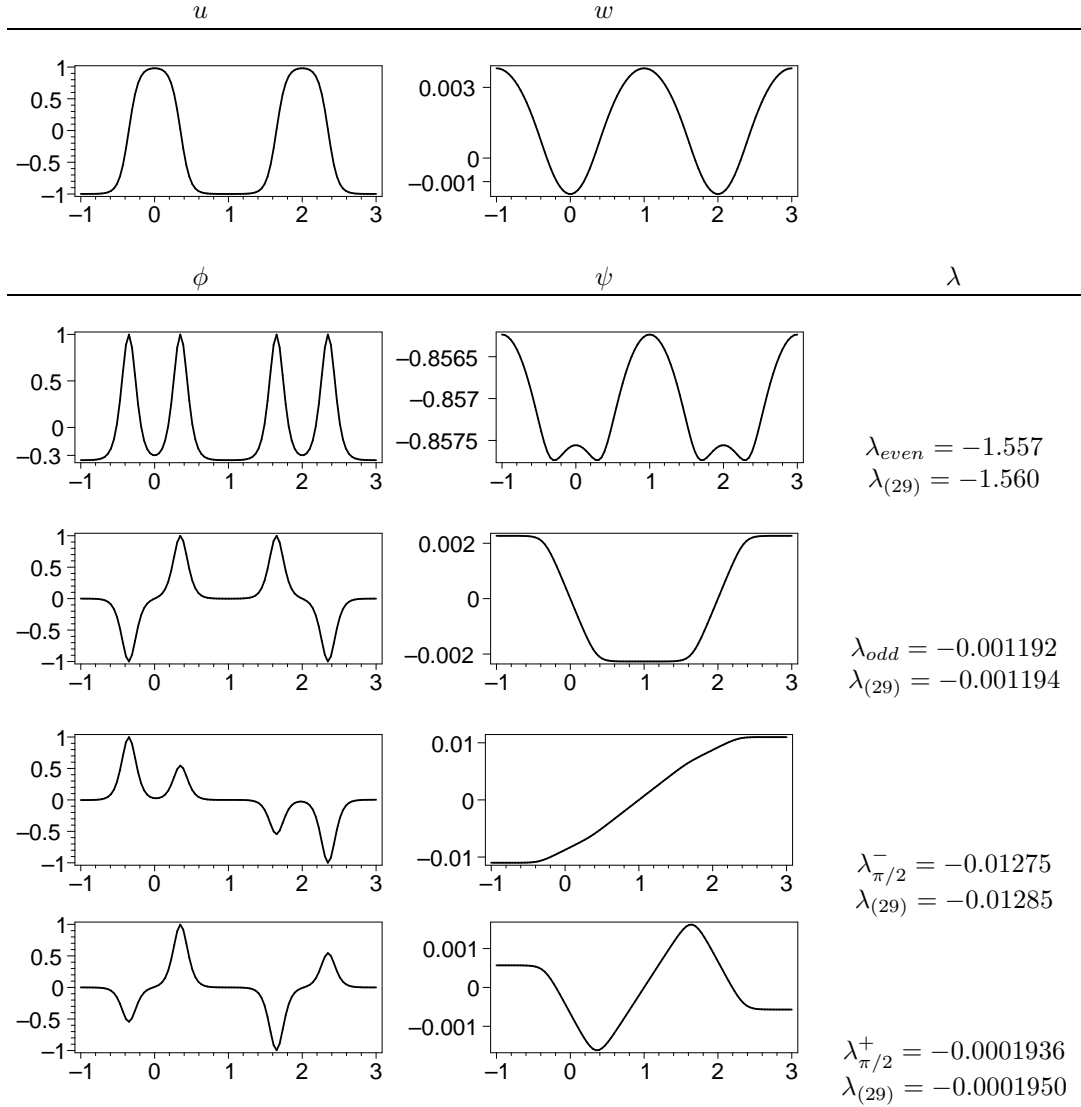


Figure 2: Top row: steady-state with two mesas. The cubic model (4) was used with $L = 1, K = 2, \varepsilon = 0.13, D = 40, \beta_0 = -0.3$. Bottom four rows: the four possible eigenfunctions and the corresponding eigenvalues. The numerical computations are described in §5. The last column shows the numerically computed value of λ as well as the asymptotic estimate $\lambda_{(29)}$ as given by (29). Excellent agreement is observed in all cases (less than 1% error).

To understand how the instability thresholds occur, consider the eigenvalue (56) first. Note that α_- is exponentially small in ε , i.e. $\alpha_- = O(e^{-c/\varepsilon})$ for some positive constant c . Thus, as ε is sufficiently decreased, $\alpha_- D$ rapidly drops off to zero and hence by assumption (23), λ_{odd} becomes negative and of $O(\frac{\varepsilon}{D})$. On the other hand, as ε is sufficiently increased (but still small), the term $\alpha_- D$ eventually overtakes the constant term $\frac{g_-^2 L}{(g_- - g_+)}$; and λ_{odd} then becomes positive, leading to an instability. In this case, the eigenvalue λ_{odd} becomes of $O(\varepsilon e^{-c/\varepsilon})$, independent of D . Similar remarks hold for λ_θ^\pm : they are of the $O(\max(\frac{\varepsilon}{D}, \varepsilon e^{-c/\varepsilon}))$ for some constant c . On the other hand, λ_{even} does not involve any boundary terms and is of $O(\varepsilon)$, always independent of D . In conclusion, $|\lambda_{even}|$ is always much bigger than the magnitude of the rest of the eigenvalues.

Figure 2 shows the actual numerical computation of the four distinct eigenvalues/eigenfunctions for the cubic model (4) with $K = 2$ (see §5 for numerical methods used). Note that ϕ is localized at the interfaces and is nearly constant elsewhere; whereas ψ has a global variation. An excellent agreement between the asymptotic results and numerical computations is observed.

Critical thresholds. To obtain instability thresholds, we set $\lambda_\theta^\pm = 0$ in Lemma 3.3; we then obtain $a - |b|^2 = 0$. Using $l = \frac{g_- L}{g_- - g_+}$ and after some algebra we obtain:

$$0 = 2\alpha_+ \alpha_- (1 - \cos \theta) D^2 - 2L \frac{g_-^2 \alpha_+ + g_+^2 \alpha_-}{g_- - g_+} D + L^2 \frac{g_+^2 g_-^2}{(g_- - g_+)^2} \quad (58)$$

which implies that $\lambda_\theta^\pm = 0$ iff $D > D_\theta$ where

$$D_\theta \sim \begin{cases} \frac{L g_+^2}{2(g_- - g_+) \alpha_-} & \text{if } \alpha_+ \ll \alpha_- \\ \frac{L g_-^2}{2(g_- - g_+) \alpha_+} & \text{if } \alpha_- \ll \alpha_+ \end{cases} \quad (59)$$

and more generally, without any assumptions on α_- and α_+ ,

$$D_\theta = \frac{L}{2(g_- - g_+) (g_-^{-2} \alpha_- + g_+^{-2} \alpha_+)} \left(\frac{1}{2} + \sqrt{\frac{1}{4} - \frac{2\alpha_+ \alpha_- (1 - \cos \theta) g_+^2 g_-^2}{4(g_-^2 \alpha_+ + g_+^2 \alpha_-)^2}} \right)^{-1}. \quad (60)$$

Note that in the limit $\varepsilon \rightarrow 0$, $\alpha_+ \ll (\gg) \alpha_- \iff \mu_-(L - l_0) < (>) \mu_+ l_0$. Together with (59, 60) this yields (27).

It is clear that D_θ is an increasing function of θ . In addition, it is also easy to verify that $\lambda_\theta^\pm < 0$ if α_\pm is decreased sufficiently, or equivalently, if D is sufficiently small: in this case the formula (29) reduces to

$$\lambda_\theta^\pm \kappa_0 \sim \frac{(g_+ - g_-) L}{D^2 (1 - \cos \theta)} \left(1 \pm \sqrt{\left[1 - 2(1 - \cos \theta) \frac{ld}{L^2} \right]} \right) - \frac{g_+ l}{D}. \quad (61)$$

On the other hand, when $K = 1$, the eigenvalues are λ_{odd} and λ_{even} , given by (56, 57). It is clear that $\lambda_{even} < 0$ for all D . On the other hand setting $\lambda_{odd} = 0$ yields the threshold (25). This completes the derivation of Principal Result 3.1.

4 Dynamics

We now derive the equations of motion of quasi-stable fronts. This will allow us to describe the dynamics of the fronts that are not necessarily in a symmetric pattern. In addition, this will also enable us to describe in more detail the aftermath of an instability of a symmetric pattern.

We assume that the pattern consists of K mesas on the interval of length $2KL$. Each mesa is bounded by two interfaces located at x_{li} and x_{ri} and we assume the ordering

$$-L < x_{l1} < x_{r1} < x_{l2} < x_{r2} < \dots < x_{lK} < x_{rK} < (2K - 1)L.$$

Moreover to leading order we assume

$$u \sim \begin{cases} u_+, & \text{if } x \in (x_{li}, x_{ri}) \text{ for some } i \in (1, K) \\ u_-, & \text{otherwise} \end{cases}$$

and near each interface we assume that

$$u(x_{li} + \varepsilon y) \sim U_0(-y), \quad u(x_{ri} + \varepsilon y) \sim U_0(y), \quad y = O(1), \quad i = 1 \dots K, \quad (62)$$

where U_0 is the heteroclinic orbit given in (16), with $U_0(y) \rightarrow u_{\pm}$ as $y \rightarrow \mp\infty$. Equation (62) can be viewed as determining the precise interface locations x_{li}, x_{ri} ; that is, for example x_{ri} is chosen to minimize the difference $|u(x_{ri} + \varepsilon y) - U_0(y)|$ for all $y \ll O(\frac{1}{\varepsilon})$. We also suppose that x_{li}, x_{ri} are slowly changing with time. In addition we define:

$$\begin{aligned} x_{ci} &:= \frac{x_{li} + x_{ri}}{2}, \quad i = 1 \dots K; \\ x_{di} &:= \frac{x_{ri} + x_{l(i+1)}}{2}, \quad i = 1 \dots K-1; \quad x_{d0} := -L, \quad x_{dK} := (2K-1)L. \end{aligned}$$

The equations of motions are derived from $2K$ solvability conditions about each interface.

First consider the interface x_{l1} . We expand

$$u(x, t) = u_0(z) + \frac{1}{D}u_1, \quad w(x, t) = w_0 + \frac{1}{D}w_1$$

where w_0 is given by (12) and

$$z = x - x_{l1}(t); \quad u_0(z) = U_0(-z/\varepsilon).$$

Expanding in terms of $\frac{1}{D}$ we obtain

$$0 = \varepsilon u_{0zz} + f(u_0, w_0); \quad (63)$$

$$-x'_{l1}(t)Du_{0x} = \varepsilon^2 u_{1zz} + f_u(u_0, w_0)u_1 + f_w(u_0, w_0)w_1; \quad (64)$$

$$0 = w_{1xx} + g(w_0, u_0). \quad (65)$$

We will see later that $x'_{l1} = O(\frac{1}{D})$ so the above expansion is indeed consistent. We multiply (64) by u_{0x} and integrate on $x \in (-L, x_{c1})$. Upon integrating by parts we obtain:

$$-x'_{l1}(t)D \int_{-L}^{x_{c1}} (u_{0x})^2 dx \sim \varepsilon^2 (u_{1z}u_{0z} - u_1u_{0zz})_{x=-L}^{x=x_{c1}} + \int_{-L}^{x_{c1}} f_w w_1 dx.$$

The boundary term is evaluated similarly as in Section 3. The end-result is,

$$\varepsilon^2 (u_{1z}u_{0z} - u_1u_{0zz})_{x=-L}^{x=x_{c1}} = 2D \left(-C_+ \mu_+^2 \exp\left(-\frac{\mu_+}{\varepsilon}(x_{r1} - x_{l1})\right) + C_- \mu_-^2 \exp\left(-\frac{2\mu_-}{\varepsilon}(L + x_{l1})\right) \right).$$

The integral terms are estimated as

$$\int_{-L}^{x_{c1}} (u_{0x})^2 dx \sim \frac{1}{\varepsilon} \int_{-\infty}^{\infty} \left(\frac{dU_0}{dy} \right)^2 dy; \quad \int_{-L}^{x_{c1}} f_w w_1 dx \sim w_1(x_{l1}) \int_{u_-}^{u_+} f_w(w_0, u) du.$$

A similar analysis is performed at each of the remaining interfaces. In this way, we obtain the following system:

$$\begin{cases} x'_{li}(t) \sim \frac{\varepsilon}{\int_{-\infty}^{\infty} U_{0y}^2 dy} \left((BT)_{li} - \frac{1}{D} w_1(x_{li}) \int_{u_-}^{u_+} f_w(w_0, u) du \right) \\ x'_{ri}(t) \sim \frac{\varepsilon}{\int_{-\infty}^{\infty} U_{0y}^2 dy} \left((BT)_{ri} + \frac{1}{D} w_1(x_{ri}) \int_{u_-}^{u_+} f_w(w_0, u) du \right) \end{cases}, \quad i = 1 \dots K \quad (66)$$

where

$$(BT)_{l1} = -2C_- \mu_-^2 \exp\left(-\frac{2\mu_-}{\varepsilon}(L + x_{l1})\right) + 2C_+ \mu_+^2 \exp\left(-\frac{\mu_+}{\varepsilon}(x_{r1} - x_{l1})\right) \quad (67)$$

$$(BT)_{li} = -2C_- \mu_-^2 \exp\left(-\frac{\mu_-}{\varepsilon}(x_{l1} - x_{r(i-1)})\right) + 2C_+ \mu_+^2 \exp\left(-\frac{\mu_+}{\varepsilon}(x_{ri} - x_{li})\right), \quad i = 2 \dots K-1 \quad (68)$$

$$(BT)_{ri} = -2C_- \mu_-^2 \exp\left(-\frac{\mu_-}{\varepsilon}(x_{ri} - x_{li})\right) + 2C_+ \mu_+^2 \exp\left(-\frac{\mu_+}{\varepsilon}(x_{l(i+1)} - x_{ri})\right), \quad i = 2 \dots K-1 \quad (69)$$

$$(BT)_{rK} = -2C_- \mu_-^2 \exp\left(-\frac{\mu_-}{\varepsilon}(x_{rK} - x_{lK})\right) + 2C_+ \mu_+^2 \exp\left(-\frac{2\mu_+}{\varepsilon}((2K-1)L - x_{rK})\right), \quad (70)$$

The constants $w_1(x_{li})$ and $w_1(x_{ri})$ are obtained by recursively solving for w_1 which satisfies:

$$w_1'' = \begin{cases} g_+, & x \in [x_{li}, x_{ri}], \quad i = 1 \dots K \\ g_- & \text{otherwise} \end{cases}; \quad w_1'(-L) = 0 = w_1'((2K-1)L).$$

To simplify the expression for w_1 , we first define the interdistances

$$m_i = \begin{cases} x_{l1} + L, & i = 0 \\ x_{l(i+1)} - x_{ri}, & i = 1 \dots K-1 \\ (2K-1)L - x_{ri}, & i = K \end{cases}; \quad p_i = x_{ri} - x_{li}, \quad i = 1 \dots K.$$

We obtain the following recursion formulae,

$$\begin{aligned} w'(x_{li}) &= \begin{cases} -g_- m_0, & i = 1 \\ w'(x_{r(i-1)}) - g_- m_i, & i = 2 \dots K \end{cases} \\ w'(x_{ri}) &= w'(x_{li}) - g_+ p_i, \quad i = 1 \dots K; \\ w(x_{li}) &= \begin{cases} w(-L) - g_- \frac{m_0^2}{2}, & i = 1 \\ w(x_{r(i-1)}) + w'(x_{r(i-1)})m_i - g_- \frac{m_i^2}{2}, & i = 2 \dots K \end{cases} \\ w(x_{ri}) &= w(x_{li}) + w'(x_{li})p_i - g_+ \frac{p_i^2}{2}, \quad i = 1 \dots K. \end{aligned}$$

Expanding, we obtain

$$\begin{aligned} w_1(x_{l1}) &= w(-L) - g_- \frac{m_0^2}{2} \\ w_1(x_{r1}) &= w(-L) - g_- \left(\frac{m_0^2}{2} + m_0 p_1\right) - g_+ \frac{p_1^2}{2} \\ w_1(x_{l2}) &= w(-L) - g_- \left(\frac{m_0^2}{2} + m_0 p_1 + m_0 m_1 + \frac{m_1^2}{2}\right) - g_+ \left(\frac{p_1^2}{2} + p_1 m_1\right) \\ w_1(x_{r2}) &= w(-L) - g_- \left(\frac{m_0^2}{2} + m_0 p_1 + m_0 m_1 + \frac{m_1^2}{2} + m_0 p_2 + m_1 p_2\right) - g_+ \left(\frac{p_1^2}{2} + p_1 m_1 + p_1 p_2 + \frac{p_2^2}{2}\right) \\ &\dots \end{aligned}$$

The general pattern is

$$\begin{aligned} w(x_{li}) &= w_1(-L) - g_- \left(\sum_{j=0}^{i-1} \sum_{k=j+1}^{i-1} m_j m_k + \sum_{j=0}^{i-1} \sum_{k=j+1}^{i-1} m_j p_k + \sum_{j=0}^{i-1} \frac{m_j^2}{2}\right) \\ &\quad - g_+ \left(\sum_{j=1}^{i-1} \sum_{k=j+1}^i p_j p_k + \sum_{j=1}^{i-1} \sum_{k=j}^{i-1} p_j m_k + \sum_{j=1}^{i-1} \frac{p_j^2}{2}\right) \end{aligned} \quad (71)$$

$$\begin{aligned} w(x_{ri}) &= w_1(-L) - g_- \left(\sum_{j=0}^{i-1} \sum_{k=j+1}^{i-1} m_j m_k + \sum_{j=0}^{i-1} \sum_{k=j+1}^i m_j p_k + \sum_{j=0}^{i-1} \frac{m_j^2}{2}\right) \\ &\quad - g_+ \left(\sum_{j=1}^i \sum_{k=j+1}^i p_j p_k + \sum_{j=1}^i \sum_{k=j}^{i-1} p_j m_k + \sum_{j=1}^i \frac{p_j^2}{2}\right). \end{aligned} \quad (72)$$

It remains to determine the constant $w_1(-L)$; this is done by considering the conservation of mass as follows. Integrating the equation for w in (1) we obtain that for all time t ,

$$g_- \sum m_j + g_+ \sum p_j = 0;$$

moreover $\sum m_j = 2KL - \sum p_j$ so that

$$\sum (x_{ri} - x_{li}) = \frac{2KLg_-}{g_- - g_+}. \quad (73)$$

Differentiating (73) with respect to t and substituting into (66) we then obtain,

$$\sum_{i=1}^K (BT)_{ri} - (BT)_{li} + \frac{1}{D} [w_1(x_{ri}) + w_1(x_{li})] \int_{u_-}^{u_+} f_w(w_0, u) du = 0. \quad (74)$$

Substituting (67-70), and (71-72) into (74) then determines the constant $w_1(-L)$.

Dynamics of a single mesa. For a single mesa, we define $x_0 = \frac{x_{l1} + x_{r1}}{2}$ to be the midpoint of the mesa. Due to mass conservation, we have

$$x_{l1} = x_0 - l, \quad x_{r1} = x_0 + l; \quad l = \frac{g_-}{g_- - g_+} L. \quad (75)$$

Substituting (75) and $x'_0 = (x'_{l1} + x'_{r1})/2$ into (66) and after some algebra we then obtain,

$$\frac{d}{dt} x_0 = \frac{\varepsilon}{2 \int_{-\infty}^{\infty} U_{0y}^2 dy} \left(-2C_- \mu_-^2 \exp\left(-\frac{2\mu_-}{\varepsilon} (L - l + x_0)\right) + 2C_+ \mu_+^2 \exp\left(-\frac{2\mu_+}{\varepsilon} (L - l - x_0)\right) - \frac{2}{D} \frac{g_-^2 \int_{u_-}^{u_+} f_w(w_0, u) du}{g_- - g_+} x_0 \right) \quad (76)$$

Note that for the special case where $C_{\pm} = C_0$; $\mu_{\pm} = \mu_0$ the formula further simplifies to

$$\frac{d}{dt} x_0 = \frac{\varepsilon}{2 \int_{-\infty}^{\infty} U_{0y}^2 dy} \left(C_0 \mu_0^2 \exp\left(-\frac{2\mu_0}{\varepsilon} (L - l)\right) \sinh\left(\frac{2\mu_0}{\varepsilon} (x_0)\right) - \frac{2}{D} \frac{g_-^2 \int_{u_-}^{u_+} f_w(w_0, u) du}{g_- - g_+} x_0 \right). \quad (77)$$

5 Numerical computations

In this section we validate our asymptotic results for the stability thresholds in Principal Result 3.1 with corresponding full numerical results computed from the eigenvalue problem (28). The predictions from these stability thresholds are then confirmed from full numerical simulations of the full PDE system (1). Let us first describe the numerical methods used.

To perform the numerical simulation of the full system (1) we used the standard software FlexPDE [29]. It uses a FEM-based approach and automatic adaptive meshing with variable time stepping. We used a global error tolerance of `errtol=0.0001` which is more than sufficient to accurately capture the interface dynamics [we also verified that changing the error tolerance did not change the solution].

To determine the eigenvalues in the spectrum of the linear eigenvalue problem (28), we have reformulated it as a boundary value problem by adjoining an extra equation $\frac{d\lambda}{dx} = 0$ as well as an extra boundary condition such as $\psi(-L) = 1$. We used the asymptotic solution derived in §2 as our initial guess. Maple's `dsolve/numeric/bvp` routine was then used to solve the resulting boundary value problem (this routine is based on a Newton-type method, see for example [30]). Unfortunately, we found that sometimes the Newton's method failed to converge, especially for problems with several interfaces. So we resorted to second method: we discretized the laplacian using the standard finite differences, thus converting (28) to a linear algebra matrix eigenvalue problem. On the other hand, this second approach is much less accurate; especially since the required eigenvalue is very small. Because of this, we used the combination of the two approaches: we used method 2 as initial guess to the boundary value problem solver. This finally converged with sufficient precision.

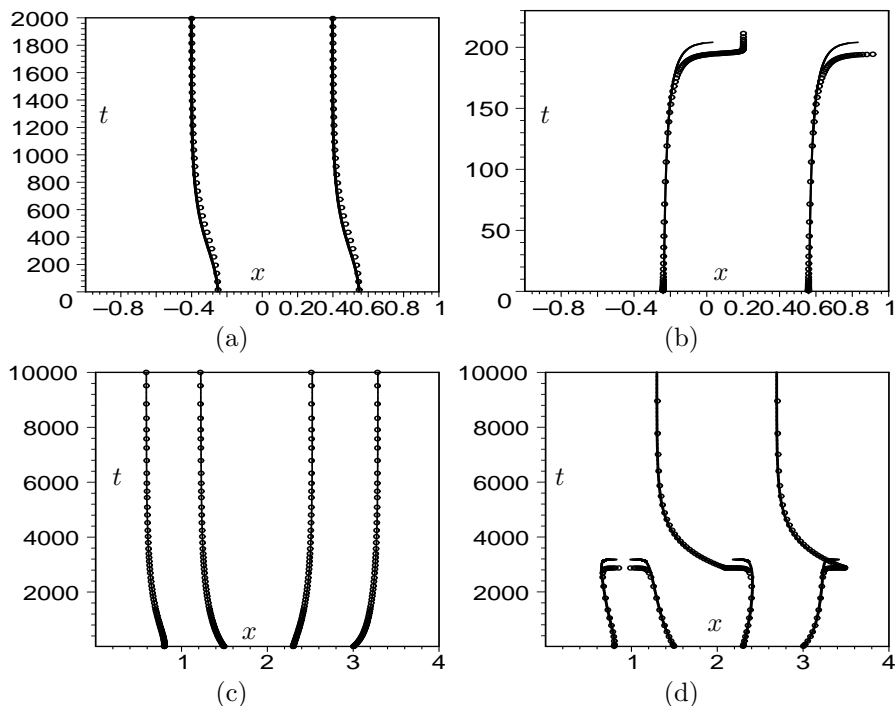


Figure 3: (a) Dynamics of a single mesa for the cubic model (4) with $\beta_0 = -0.2$; $\varepsilon = 0.22$, $D = 20$, $L = 1$. Vertical axis is time, horizontal axis is space. The contour $u = 0$ is shown. Solid lines are the asymptotic results derived in §4. Dots represent the output of the full numerical simulation of (4) using FlexPDE. The initial conditions are given by (90) with $x_0 = 0.15$. (b) Same as in (a), but $x_0 = 0.16$. (c) Dynamics of two-mesas. The parameters are $K = 2$, $L = 1$ (so that $x \in [0, 4]$); $\beta_0 = -0.3$, $\varepsilon = 0.13$, $D = 70$. Initial interface locations are 0.8, 1.5, 2.3, 3.0. (d) Same as (c) except that $D = 85$.

5.1 Cubic model

We now specialize our results to the cubic model (4),

$$f = 2(u - u^3) + w; \quad g = \beta_0 - u.$$

Let us first consider a symmetric mesa solution on interval $[-L, L]$, with its maximum at $x = 0$. For such a solution, we find

$$w_0 = 0; \quad u_- = -1, \quad u_+ = +1; \quad U_0(y) = -\tanh(y); \quad (78)$$

$$g_+ = \beta_0 - 1, \quad g_- = \beta_0 + 1; \quad (79)$$

$$\int_{-\infty}^{\infty} U_{0y}^2 dy = \frac{4}{3}; \quad \int_{u_-}^{u_+} f_w(u, w_0) du = 2; \quad (80)$$

$$l_0 = \frac{\beta_0 + 1}{2} L; \quad l_1 = 0; \quad (81)$$

$$\mu_{\pm} = 2; \quad C_{\pm} = 2; \quad \alpha_{\pm} = 32 \frac{1}{\varepsilon} \exp\left(-\frac{2}{\varepsilon} (1 \pm \beta_0) L\right). \quad (82)$$

The condition (14) simply states that $0 < l_0 < L$; this implies $|\beta_0| < 1$. One of the advantages of using the cubic model as a test case is that due to symmetry, the correction l_1 to the interface location is $l_1 = 0$. This means that the asymptotic results are expected to be very accurate.

We obtain the following expressions for λ_{odd} and λ_{even} :

$$\lambda_{even} \sim -12\varepsilon \quad (83)$$

$$\lambda_{odd} \sim -\frac{3(\beta_0 + 1)^2 L\varepsilon}{4D} + 96 \exp\left(-\frac{2L}{\varepsilon}(1 - \beta_0)\right) \quad (84)$$

The even eigenvalue λ_{even} is always stable. Alternatively, the odd eigenvalue λ_{odd} becomes unstable as D is increased past the critical threshold D_1 which is given by

$$D_1 = \frac{(\beta_0 + 1)^2 L\varepsilon}{128} \exp\left(\frac{2L}{\varepsilon}(1 - \beta_0)\right) \quad (85)$$

with $\lambda_{odd} < 0$ when $D < D_1$ and with $\lambda_{odd} > 0$ when $D > D_1$. In terms of D_1 , we have

$$\lambda_{odd} \sim -\frac{3(\beta_0 + 1)^2 L\varepsilon}{4} \left(\frac{1}{D} - \frac{1}{D_1}\right).$$

and the equations of motion for a single mesa become

$$\frac{dx_0}{dt} = \frac{3(\beta_0 + 1)^2}{4} L\varepsilon \left(\frac{1}{D_1} \frac{\varepsilon}{4} \sinh\left(\frac{4x_0}{\varepsilon}\right) - \frac{1}{D} x_0\right), \quad (86)$$

where $x_0 = \frac{x_{l1} + x_{r1}}{2}$ is the center of the mesa. Note that

$$\left. \frac{\partial}{\partial x_0} \left(\frac{dx_0}{dt}\right) \right|_{x_0=0} = \lambda_{odd}$$

so that the linearization of the equations of motion around the symmetric equilibrium agrees with the full linearization of the original PDE. We remark that the equilibrium $x_0 = 0$ undergoes a pitchfork bifurcation and becomes unstable as D increases past D_1 .

For K symmetric mesas on the interval of length $2R$, we have

$$L = R/K$$

and the thresholds (27) become:

$$D_K \sim \begin{cases} \frac{(1 - \beta_0)^2 \frac{R}{K} \varepsilon}{128} \exp\left(\frac{2R}{\varepsilon K}(1 + \beta_0)\right), & \text{if } \beta_0 < 0; \\ \frac{(1 + \beta_0)^2 L\varepsilon}{128} \exp\left(\frac{2R}{\varepsilon K}(1 - \beta_0)\right), & \text{if } \beta_0 > 0 \end{cases}; \quad K \geq 2 \quad (87)$$

Finally, if we take the ‘‘inverted’’ mesa with $u \sim +1$ near the boundaries, by changing the variables $u \rightarrow -u$, $w \rightarrow -w$, the model remains the same except β_0 is replaced by $-\beta_0$. Thus the stability thresholds for the inverted mesa are

$$D_1^i = \frac{(1 - \beta_0)^2 L\varepsilon}{128} \exp\left(\frac{2L}{\varepsilon}(1 + \beta_0)\right) \quad (88)$$

$$D_K^i \sim \begin{cases} \frac{(1 - \beta_0)^2 \frac{R}{K} \varepsilon}{128} \exp\left(\frac{2R}{\varepsilon K}(1 + \beta_0)\right), & \text{if } \beta_0 < 0; \\ \frac{(1 + \beta_0)^2 \frac{R}{K} \varepsilon}{128} \exp\left(\frac{2R}{\varepsilon K}(1 - \beta_0)\right), & \text{if } \beta_0 > 0 \end{cases}; \quad K \geq 2 \quad (89)$$

We now numerically validate our asymptotic results by direct comparison with full numerical simulation of the system (4).

Mesa dynamics: single mesa. Choose $L = 1, \varepsilon = 0.22$ and $\beta_0 = -0.2$. From (85) we then get $D_c = 60.138$. Now suppose that $D = 20$. Then the ODE (86) admits three equilibria: $x_0 = 0$ (stable) and $x_{\pm} = \pm 0.156$ (both unstable). We now solve the full system. We take initial conditions to be

$$u(x, 0) = \tanh\left(\frac{(x - x_0) + l}{\varepsilon}\right) - \tanh\left(\frac{(x - x_0) - l}{\varepsilon}\right) - 1; \quad w(x, 0) = 0. \quad (90)$$

This corresponds to a mesa solution of length l centered at x_0 . Thus if $x_0 \in (-0.156, 0.156)$ then we expect the mesa to move to the center of the domain and stabilize there. On the other hand, if $x_0 > 0.156$ then the mesa will move to the right until it merges with the right boundary. In Figure 3, we plot the numerical simulations for $x_0 = 0.150$ and $x_0 = 0.160$. The observed behaviour agrees with the above predictions.

Dynamics of two-mesa solution. Here we consider a two-mesa solution. We take the domain $x \in [0, 4]$ (i.e. $L = 1, K = 2$) and take $\beta_0 = -0.3, \varepsilon = 0.13$. From (81), we get $l = 0.35$ so that the symmetric equilibrium location of the interfaces are 1 ± 0.35 and 3 ± 0.35 which yields $0.65, 1.35, 2.65, 3.35$. According to (87), the two-mesa symmetric configuration is stable provided that $D < 82$, and is unstable otherwise. To verify this, we solve the full system with initial interface locations given by $0.8, 1.5, 2.3, 3.0$. These are relatively close to the symmetric equilibrium. We found that when $D < 80$, such a configuration converges to the symmetric two-mesa equilibrium; however it is unstable if $D > 80$ – see Figure 3(c,d). This is in good agreement with the theoretical threshold $D_2 = 82$. Moreover, the instability triggers a “mass exchange”, whereby one of the mesas grows in size whereas the other shrinks by the same amount, until only one mesa is left. This is clearly visible in Figure 3(d).

Next we also compute the four eigenvalues for several values of D , and compare to asymptotic results, shown in Figure 4. An excellent agreement is once again observed, including the crossing of zero for $\lambda_{\pi/2}^+$ at $D = 82$.

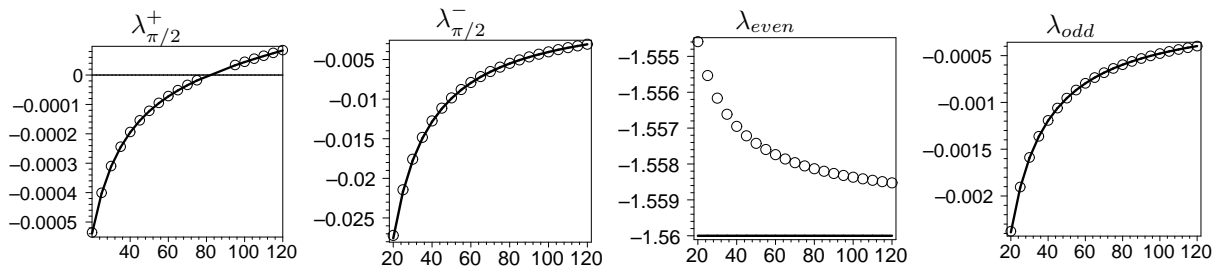


Figure 4: The four eigenvalues of the two-mesa pattern of (4) as a function of D . Other parameters are as in Figure 3(c,d). Circles represent numerical computations of (28); lines are the asymptotic results given by (29). Excellent agreement is observed, including the crossing of $\lambda_{\pi/2}^+$ at $D = D_2 = 82$.

The transitional case of $\beta_0 = 0$. This is the degenerate case for which the formula (87) does not apply. In this case, $\alpha_+ = \alpha_-$ and the formula (27) reduces to

$$D_K \sim \frac{L}{256 \cos^2\left(\frac{\pi}{4K}\right)} \varepsilon \exp(2L/\varepsilon); \quad \beta_0 = 0, \quad K \geq 1. \quad (91)$$

(this formula is also valid when $K = 1$, as can be verified by comparing it to (85)). Note that this is also qualitatively different from $\beta_0 \neq 0$, in that D_K actually depends on K when $\beta_0 = 0$. To validate (91) numerically, we set $\varepsilon = 0.17, L = 1, \beta_0 = 0$. Formula (91) then yields the asymptotic thresholds $D_1 = 170.8, D_2 = 100.1, D_3 = 91$. Next, we have computed the eigenvalues $\lambda_{\pm}^{\pi/K}$ explicitly using the full formulation (28) for $K = 1, 2, 3$ several different D and for ε, L as above. These are shown in Figure 5. An excellent agreement can be observed with the predicted threshold values. For example for $D = 95$, a two-mesa steady state on the interval $[-1, 3]$ of size 4 is stable but a three-mesa steady state on the interval $[-1, 5]$ of size 6 is not.

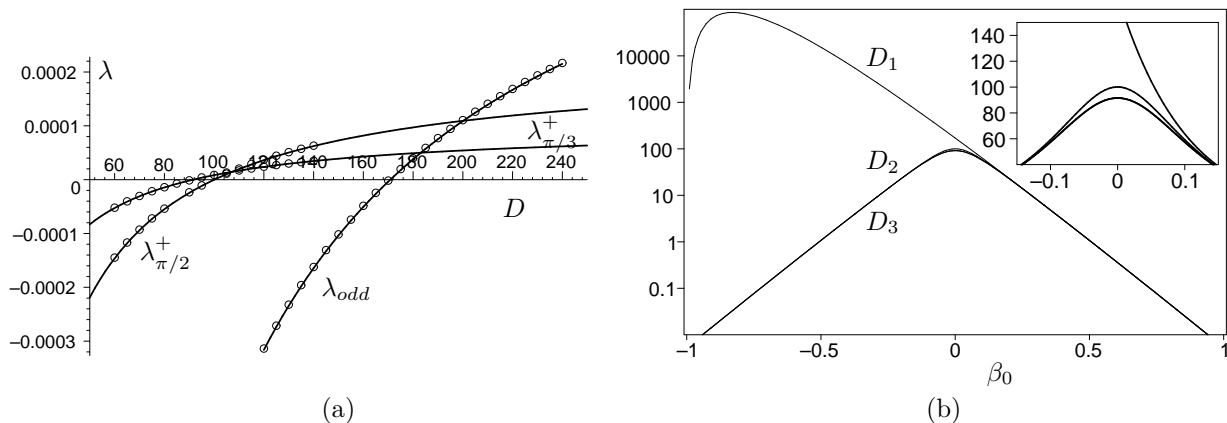


Figure 5: Instability thresholds of the K -mesa pattern in the cubic model with $K = 1, 2$ and 3 . (a) $L = 1, \varepsilon = 0.17, \beta_0 = 0$. Circles show λ as computed by numerically solving the full formulation (28) for different values of D and the three different modes, as indicated. Solid curves are the asymptotic approximations for λ as given by (29). The K -mesa pattern is unstable for $D > D_K$ where $D_1 = 171, D_2 = 100, D_3 = 91$. (b) The graph of D_K versus β_0 with $L = 1, \varepsilon = 0.17$, as given by Principal Result 3.1 (note the logarithmic scale). The insert shows the zoom near $\beta_0 = 0$.

Boundary-mesa versus interior mesas. Let us now compare the stability properties of interior mesas versus patterns with half-mesas attached to the boundary. The latter are equivalent to an “inverted mesa” patterns. This situation is shown in the Figure 6.

Fix $\varepsilon = 0.15, L = 1$. Moreover $\beta_0 = -0.1 < 0$ so that the roof of the mesa occupies more space than its floor ($l = 0.45 < 1/2$). In this case, the instability threshold for a single mesa is (85), $D_1 \sim 2223$ and for the inverted mesa it is (88), $D_1^i = 230$. Moreover the instability thresholds for K interior mesas on the interval $2LK$ with $K > 1$ is also (87) $D_K \sim 230$. This threshold is also the same for two boundary mesas or K inverted mesas (89).

Despite the fact that the stability analysis in section 3 required retaining exponentially small terms, the numerical results have shown that the stability thresholds from the asymptotic theory can be used very effectively, and in excellent agreement with full numerical simulations, even when ε is not very small. There are two possible explanations for this. The first explanation is specific to the cubic model: due to the symmetry of the nonlinear term, the first correction l_1 to the interface location is identically zero. The second explanation is that the “effective” small quantity is $\exp(-c/\varepsilon)$, which can be very small even if ε is only moderately small.

5.2 Model of Belousov-Zhabotinskii reaction in water-in-oil microemulsion

The cubic model is unusual in the sense that due to the symmetry of the interface, the correction to interface length l_1 of Proposition 2.1 is zero. To see the more usual case when it is not – and a dramatic effect that it can have on the accuracy of asymptotics – consider the Belousov-Zhabotinskii model (5):

$$f(u, w) = -f_0 \frac{u - q}{u + q} + wu - u^2; \quad g(u, w) = 1 - uw; \quad q \ll 1. \quad (92)$$

As was done in [16], in the limit $q \ll 1$, the condition (12) reduces to

$$\int_0^{u_+} (-f_0 + w_0 u - u^2) du \sim 0 \sim -f_0 + w_0 u_+ - u_+^2$$

and we obtain to leading order,

$$u_- \sim 0; \quad u_+ \sim \sqrt{3f_0}; \quad w_0 \sim 4\sqrt{f_0/3} \quad \text{as } q \rightarrow 0.$$

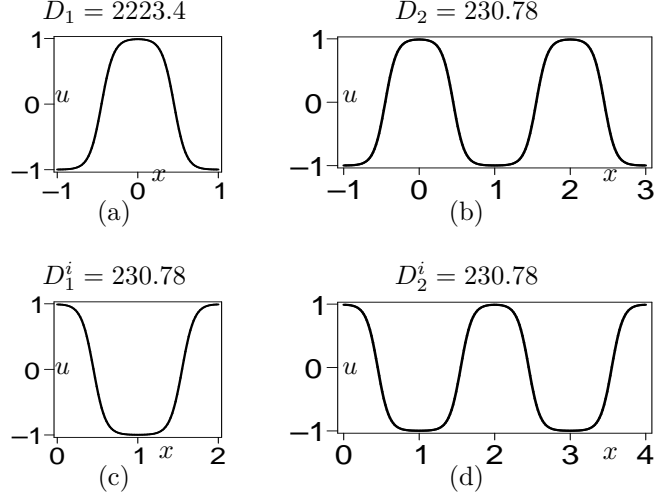


Figure 6: (a) Single Interior mesa (b) Two interior mesas (c) Double boundary half-mesas, or an inverted single interior mesa (d) Two half-mesas at the boundaries and one interior mesa, or an inverted two-mesa pattern. In all four cases, $\beta_0 = -0.1$ and $\varepsilon = 0.15$. The instability threshold for D is given above the graph.

(in fact, $u_- = O(q) \ll 1$). To leading order, the profile U_0 then solves $U_0'' - f_0 + 4\sqrt{f_0/3}U_0 - U_0^2 = 0$ for $y < 0$; with $U_0(0) = 0 = U_0'(0)$ and $U_0(y) = 0$ for $y > 0$ and $U_0 \rightarrow u_+$ as $y \rightarrow -\infty$. We then obtain

$$U_0 \sim \begin{cases} \sqrt{3f_0} \tanh^2 \left(3^{-1/4} f_0^{1/4} 2^{-1/2} y \right), & y < 0 \\ 0, & y > 0 \end{cases}.$$

and

$$g_- = 1, \quad g_+ \sim 1 - 4f_0$$

$$l_0 = \frac{L}{4f_0}.$$

Next we compute the correction l_1 to the interface position using (19). We have

$$\begin{aligned} & \int_{-\infty}^0 [g(U_0(y), w_0) - g_+] dy \\ &= \int_{-\infty}^0 4f_0 - 4f_0 \tanh^2 \left(3^{-1/4} f_0^{1/4} 2^{-1/2} y \right) dy \\ &= 4f_0 \int_0^{\infty} \operatorname{sech}^2 \left(3^{-1/4} f_0^{1/4} 2^{-1/2} y \right) dy = 3^{1/4} 2^{1/2} 4f_0^{3/4} \end{aligned}$$

so that

$$l_1 = 3^{1/4} 2^{1/2} f_0^{-1/4}.$$

Finally, we have

$$U_0 \sim \sqrt{3f_0} \tanh^2 \left(3^{-1/4} f_0^{1/4} 2^{-1/2} y \right) \sim \sqrt{3f_0} \left(1 - 4 \exp(3^{-1/4} f_0^{1/4} 2^{1/2} y) \right) \quad \text{as } y \rightarrow -\infty$$

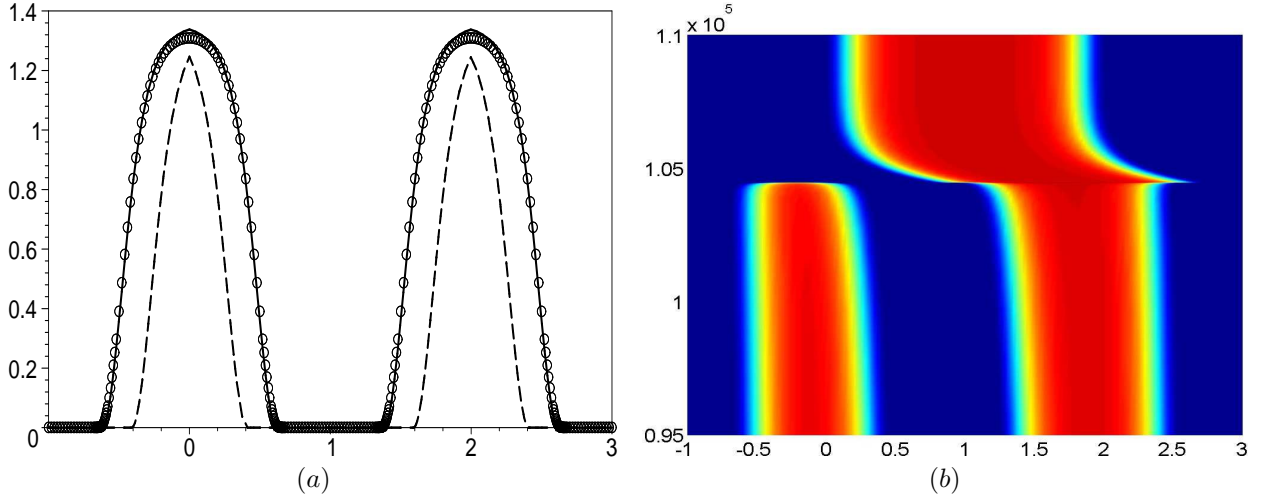


Figure 7: (a) A stable two-mesa solutions to Belousov-Zhabotinskii model (5). Parameter values are $D = 100$, $\varepsilon = 0.1$, $q = 0.001$ and $f_0 = 0.61$. Circles show the full numerical solution. The solid line shows the asymptotic approximation as computed in Proposition 2.1, with the mesa half-length l computed to two orders. The dashed line is the same approximation, except l_1 is set to zero. (b) Time evolution in the BZ model. Parameter values are the same as in (a), except for $f_0 = 0.63$. Initial conditions were given in the form of a two-mesa asymptotic solution, but shifted to the left by 0.05.

so that

$$\begin{aligned}
C_+ &= 4\sqrt{3f_0}; \quad \mu_+ = 3^{-1/4} f_0^{1/4} 2^{1/2}; \\
\int_{u_-}^{u_+} f_w du &= \frac{u_+^2}{2} = \frac{3f_0}{2}; \\
\alpha_+ &= 64 \cdot 3^{-3/4} f_0^{3/4} 2^{3/2} \exp(-2\mu_+ l_1) \frac{1}{\varepsilon} \exp\left(-\frac{2\mu_+}{\varepsilon} l_0\right) \\
&= 64 \cdot 3^{-3/4} f_0^{3/4} 2^{3/2} \exp(-4) \frac{1}{\varepsilon} \exp\left(-\frac{2^{-1/2} 3^{-1/4}}{\varepsilon f_0^{3/4}} L\right)
\end{aligned}$$

On the other hand, $\mu_- = O(1/q) \gg \mu_+$, so that the critical threshold given by (27) becomes

$$D_K = C_0 \varepsilon (1 - 4f_0)^2 f_0^{-7/8} \exp\left(\frac{2^{-1/2} 3^{-1/4}}{\varepsilon f_0^{3/4}} L\right); \quad C_0 \equiv e^4 3^{3/4} 2^{-21/2} = 0.085942, \quad K \geq 2 \quad (93)$$

To verify this formula numerically, we set $D = 100$, $\varepsilon = 0.1$, $q = 0.001$, $L = 1$ and $K = 2$. Next we solved (1) for several different values of f_0 , with initial conditions given by the two-mesa steady state approximation on the interval $[-1, 3]$, perturbed by a small shift of size 0.1. We found the two-mesa state was unstable with $f_0 \geq 0.62$ but became stable when we took $f_0 \leq 0.61$ – see Figure 7. On the other hand, the threshold value as predicted by (93) with above parameter values and $D_K = D$ is $f_0 = 0.6124$. Thus we obtain an excellent agreement between the asymptotic theory and direct numerical simulations.

In Figure 7(a), the approximation with and without l_1 to the steady state is shown. We remark that it was essential to compute the correction l_1 to the mesa width; if we were to set $l_1 = 0$ the constant $C_0 = 0.085942$ in (93) would be replaced by 0.00157, a dramatic difference by a factor of $e^4 \approx 50$. In figure 7(b), the two-mesa equilibrium is shown to be unstable for $f_0 = 0.63$, though the instability is very slow and the two-mesa solution persists until about $t \approx 10^5$. Such slow instability is an example of *metastability*.

6 Discussion

We have examined in detail the route to instability of the K -mesa pattern of (1) as the diffusion coefficient D is increased. The onset of instability occurs for exponentially large D ; it is well known that such solution is unstable for the shadow system case $D \rightarrow \infty$, see [12]. We have computed explicit instability thresholds D_K given by Principal Result 3.1; as well as mesa dynamics when D is large.

The instability thresholds are closely related to the *coarsening* phenomenon – see Figure 1 for example. This was previously analysed for the Brusselator in [17], where the authors have guessed at the formula for D_K , $K > 1$ as given in Principal Result 3.1 by constructing the so-called asymmetric patterns, and without computing the eigenvalues. The formula for D_K appears to correspond precisely to the point at which the asymmetric solution bifurcates from the symmetric branch [17]. This is indeed the case when $\mu_{+l} \neq \mu_{-(L-l)}$, i.e. $O(\alpha_+) \neq O(\alpha_-)$. In particular, this is true when either l or $L-l$ is sufficiently small. However the study of asymmetric patterns *cannot predict* the instability thresholds if $\mu_{+l} = \mu_{-(L-l)}$: in this case, the formula (27) for D_K actually depends on K , unlike the former case; whereas the construction of asymmetric patterns is K independent. So in the case $\mu_{+l} = \mu_{-(L-l)}$, the full spectral analysis is unavoidable.

There are some similarities between the instability thresholds for mesa patterns computed here, and instability thresholds for Gierer-Meinhardt system computed in [31], [32]. [In [31], a singular perturbation and matrix algebra approach was used; in [32] an approach using Evans functions and Floquet theory was used. In this paper we have used a combination of both singular perturbation methodology and Floquet theory.] To be concrete, consider the “standard” GM system,

$$a_t = \varepsilon^2 a_{xx} - a + a^2/h; \quad 0 = Dh_{xx} - h + a^2. \quad (94)$$

Unlike the K mesa patterns considered in this paper, the steady state for GM system considered in [31] consists of K spikes, concentrated at K symmetrically spaced points. The authors derived a sequence of thresholds

$$D_1^* = \varepsilon^2 \exp(2/\varepsilon)/125 \quad (95)$$

$$D_K^* = \frac{1}{[K \ln(\sqrt{2} + 1)]^2}, \quad K \geq 2 \quad (96)$$

such that K spikes on the interval $[-1, 1]$ are stable if $D < D_K^*$ and unstable if $D > D_K^*$. By comparison, letting $L = \frac{1}{K}$, and considering only the case $\mu_{+l} < \mu_{-(L-l)}$, the thresholds in Principal Result 3.1 become

$$D_1 = O\left(\frac{\varepsilon}{K} \exp\left(\frac{1}{K\varepsilon} \frac{2\mu_- g_+}{g_+ - g_-}\right)\right);$$

$$D_K = O\left(\frac{\varepsilon}{K} \exp\left(\frac{1}{K\varepsilon} \frac{2\mu_+ g_-}{g_- - g_+}\right)\right) \quad \text{if } \mu_{+l} < \mu_{-(L-l)}, \quad K > 1.$$

Thus D_K is exponentially large in ε for all K , whereas D_K^* is $O(1)$ for $K > 1$ and exponentially large for $K = 1$.

We remark that the GM model with saturation (7) exhibits mesa patterns when the saturation is sufficiently large, but exhibits spikes when saturation is small. It is an interesting open question to elucidate the transition mechanism whereby a mesa can become a spike and how the various instability thresholds change from being exponentially large to algebraically large as saturation is decreased.

The coarsening phenomenon observed in reaction-diffusion systems is also reminiscent of Ostwald ripening in thin fluids – see for example [33], [34] and references therein.

Throughout the paper, we used the methods of formal asymptotics and no attempt has been made to provide a rigorous justification. There are several techniques available to provide a more rigorous foundation, such as the renormalization group method [35], [36] (for dynamics) or Lyapunov-Schmidt reduction [37] (for steady states and stability computations). One of the difficulties here is the presence of exponentially small (or large) quantities. It is an open problem make our results rigorous.

In two dimensions, another instability occurs for radially symmetric spot solutions, see for example [16], [13], [38]. However the instability computed there is initiated because of the curvature of the spot and the instability thresholds occur when $D = D_c = O(1/\varepsilon)$, with the spot being *stable* if $D > D_c$ and *unstable* if $D < D_c$. Such an instability leads to the deformation of the spot into a peanut-like shape and has no analogy to the one dimensional instabilities studied in this paper. Yet, just like in one dimension, it is expected that an interior two-dimensional spot is unstable for the shadow system $D \rightarrow \infty$. This suggests that there exists in two dimensions a number $D_{c'} > D_c$ such that one spot is stable when $D \in (D_c, D_{c'})$ and is unstable otherwise. We anticipate that just like in the one dimensional case, $D_{c'}$ would be exponentially large; the exact computation remains an open problem (but see [39] for related computations for a spike in GM model).

7 Acknowledgements

We thank the referees for many careful remarks and useful suggestions which have improved the paper considerably. R.M. would like to thank the support from The Patrick F. Lett Graduate Students Bursary, Dalhousie. T.K. would like to thank the support from NSERC Discovery grant, Canada.

References

- [1] Y. Nishiura and H. Fujii. Stability of singularly perturbed solutions to systems of reaction-diffusion equations. *SIAM J.Math.Anal.*, 18:1726–1770, 1987.
- [2] Y. Nishiura and M. Mimura. Layer oscillations in reaction-diffusion systems. *SIAM J.Appl. Math.*, 49:481–514, 1989.
- [3] C. B. Muratov and V. Osipov. Scenarios of domain pattern formation in a reaction-diffusion system. *Phys.Rev.E*, 54:4860–4879, 1996.
- [4] J. Rubinstein, P. Sternberg, and J. B. Keller. Fast reaction, slow diffusion, and curve shortening. *SIAM J.Appl.Math*, 49(1):116–133, Feb 1989.
- [5] R. E. Goldstein, D. J. Muraki, and D. M. Petrich. Interface proliferation and the growth of labyrinths in a reaction-diffusion system. *Phys. Rev. E*, 53(4):3933–3957, 1996.
- [6] G. Nicolis and I. Prigogine. *Self-organization in Non-Equilibrium Systems*. Wiley Interscience, New York, 1977.
- [7] J. D. Murray. *Mathematical Biology*. Springer-Verlag, Berlin, 1989.
- [8] B. S. Kerner and V. V. Osipov. *Autosolitons: a New Approach to Problems of Self-Organization and Turbulence*. Kluwer, Dordrecht, 1994.
- [9] R. Kapral and K. Showalter, editors. *Chemical waves and patterns*. Kluwer, Dordrecht, 1995.
- [10] M. Taki M. Tlidi and T. Kolokolnikov, editors. Dissipative localized structures in extended systems. *Chaos Focus issue*, 17, 2007.
- [11] T. Kolokolnikov, M. Ward, and J. Wei. Self-replication of mesa patterns in reaction-diffusion models. *Physica D*, Vol, 236(2):104–122, 2007.
- [12] W. M Ni, P. Poláčik, and E. Yanagida. Monotonicity of stable solutions in shadow systems, *trans. A.M.S*, Vol, 352(12):5057–5069, 2001.
- [13] C. Muratov and V. V. Osipov. General theory of instabilities for patterns with sharp interfaces in reaction-diffusion systems. *Phys, Rev. E*, 53(4):3101-3116, 1996.

- [14] A. Kaminaga, V. K. Vanag, and I. R. Epstein. A reaction-diffusion memory device. *Angewandte chemie*, 45:3087–3089, 2006.
- [15] A. Kaminaga, V. K. Vanag, and I. R. Epstein. Black spots in a surfactant-rich Belousov-Zhabotinsky reaction dispersed in a water-in-oil microemulsion system. *J. Chem. Phys.*, 122:061747, 2005.
- [16] T. Kolokolnikov and M. Tlidi. Spot deformation and replication in the two-dimensional Belousov-Zhabotinski reaction in a water-in-oil microemulsion system. *Phys.Rev.Lett.*, 98:188303, 2007.
- [17] T. Kolokolnikov, T. Erneux, and J. Wei. Mesa-type patterns in the one-dimensional Brusselator and their stability. *Physica D*, 214:63–77, 2006.
- [18] H. Meinhardt. Models of biological pattern formation, Academic press. *London*, 1982.
- [19] H. Meinhardt. The algorithmic beauty of sea shells, Springer-verlag. *Berlin*, 1995.
- [20] A. J. Koch and H. Meinhardt. Biological pattern formation: from basic mechanisms to complex structures. *Rev. Modern Physics*, 66(4):1481–1507, 1994.
- [21] T. Kolokolnikov, M. Ward, W. Sun, and J. Wei. The stability of a stripe for the Gierer-Meinhardt model and the effect of saturation. *SIAM J. Appl. Dyn. Systems*, 5(2):313–363, 2006.
- [22] I Lengyel and IR Epstein. Modeling of Turing structures in the chlorite-iodide-malonic acid-starch reaction system. *Science, Vol*, 251(4994):650–652, 1991.
- [23] W. Ni and M. Tang. Turing patterns in the Lengyel-Epstein system for the CIMA reaction. *Trans. AMS*, 357(10):3953–3969, 2005.
- [24] M. Mimura, Y. Nishiura, A. Tesei, and T. Tsujikawa. Coexistence problem for two competing species models with density-dependent diffusion. *Hiroshima Math J.*, 14(2):425–449, 1984.
- [25] E. Meron, H. Yizhaq, and E. Gilad. Localized structures in dryland vegetation: forms and functions. *Chaos*, 17:037109, 2007.
- [26] T. Hillen and K. J. Painter. A user’s guide to PDE models for chemotaxis. *J Math Biol.*, 58(1):183–217, 2009.
- [27] R. Choksi and X. Ren. On the derivation of a density functional theory for microphase separation of diblock copolymers,. *J. Stat. Phys*, 113(1):151–176, 2003.
- [28] R. McKay and T. Kolokolnikov, Interface oscillations in reaction-diffusion systems beyond the Hopf bifurcation, submitted.
- [29] FlexPDE software, see www.pdesolutions.com.
- [30] U. Ascher, R. Christiansen, and R. Russell. Collocation software for boundary value ode’s. *Math Comp.*, 33:659–579, 1979.
- [31] D. Iron, M. J. Ward, and J. Wei. The stability of spike solutions to the one-dimensional gierer-meinhardt model. *Physica D*, 150:25–62, 2001.
- [32] H. van der Ploeg, and A. Doelman, Stability of spatially periodic pulse patterns in a class of singularly perturbed reaction-diffusion equations. *Indiana Univ. Math. J.* 54(5):1219–1301, 2005.
- [33] K.B. Glasner and T.P. Witelski. Collision versus collapse of droplets in coarsening of dewetting thin films. *Physica D, Vol*, 209:80–104, 2005.
- [34] F. Otto, T. Rump, and D. Slepcev. Coarsening rates for a droplet model: rigorous upper bounds. *SIAM J.Math. Analysis*, 38(2):503-529, 2007.

- [35] K. Promislow. A Renormalization Method for Modulational Stability of Quasi-Steady Patterns in Dispersive Systems, *SIAM J. Math. Anal.* 33(6):1455-1482, 2002.
- [36] A. Doelman, T.J. Kaper and K. Promislow. Nonlinear asymptotic stability of the semistrong pulse dynamics in a regularized Gierer-Meinhardt model, *SIAM J. Math. Anal.* 38(6):1760-1787, 2007.
- [37] J. Wei and M. Winter. Multi-Peak Solutions for a Wide Class of Singular Perturbation Problems, *J. London Math. Soc.*, 59 (2): 585-606, 1999.
- [38] C. Muratov. Theory of domain patterns in systems with long-range interactions of Coulomb type, *Phys.Rev.E*, 66(2): 066108.1-066108.25, 2002.
- [39] T. Kolokolnikov and M. J. Ward. Bifurcation of spike equilibria in the near-shadow Gierer-Meinhardt model. *Discrete and Continuous Dynamical Systems B*, pages 1033–1064, 4 2004.